Custom-design of intrinsically antimicrobial polyurethane hydrogels as multifunctional injectable delivery systems for mini-invasive wound treatment

Engineered Regeneration 2 (2021) 263–278

Contents lists available at ScienceDirect

Engineered Regeneration

journal homepage: http://www.keaipublishing.com/en/journals/engineered-regeneration/

Custom-design of intrinsically antimicrobial polyurethane hydrogels as multifunctional injectable delivery systems for mini-invasive wound treatment

Rossella Laurano[a], Valeria Chiono[a], Chiara Ceresa[b], Letizia Fracchia[b], Alice Zoso[a], Gianluca Ciardelli[a], Monica Boffito[a,*]

[a] Mechanical and Aerospace Engineering Department, Politecnico di Torino, Corso Duca degli Abruzzi 24, Torino 10129, Italy
[b] Department of Pharmaceutical Sciences, Università del Piemonte Orientale A. Avogadro, Largo Guido Donegani 2, Novara 28100, Italy

ARTICLE INFO

Keywords:
Antimicrobial poly(ether urethane)s
Drug delivery systems
Injectable formulations
Antibiotic-free treatments
Wound healing
Thermosensitive hydrogels

ABSTRACT

Effective management of hard-to-close skin wounds is a challenging issue due to several co-morbidities in affected patients. Particularly, infections represent a major obstacle in wound healing. The design of efficient wound treatments thus represents an urgent need. Injectable drug delivery hydrogels with intrinsic antimicrobial and antifungal properties were herein designed for perspective application in the mini-invasive treatment of hard-to-close wounds. First, an amphiphilic polyurethane was synthesized from Poloxamer® 407 macrodiol and N-Boc diethanolamine chain extender (DHP407, $\bar{M}_w$=33 kDa). Chain-extension reaction step was optimized to maximize the formation of -NH groups along the polymer chains ($4.5 \times 10^{20} \pm 1.8 \times 10^{19}$ –NH groups/$g_{polymer}$), after Boc-caging group removal (D-DHP407). DHP407 and D-DHP407 water-based solutions were thermosensitive with slightly different Critical Micellar Concentration (17.5 μg/mL vs. 19.7 μg/mL) and cluster hydrodynamic diameter (235.6 ± 19.9 nm vs. 260.1 ± 20.5 nm), and similar Critical Micellar Temperature (22.5 °C vs. 23.1 °C). A polyurethane solution concentration (15% w/V) was selected by tube-inverting test and rheological analysis showing injectability, as evidenced by sol-to-gel transition at 27.7 ± 0.6 °C for DHP407 and 29.7 ± 0.6 °C for D-DHP407, within few minutes, at similar gelation kinetics. DHP407 and D-DHP407 hydrogels showed controlled release of Bovine Serum Albumin (BSA) model protein (1 mg/mL), with no burst phenomena. BSA released from DHP407 and D-DHP407 hydrogels at 24 h was 33.7 ± 5.0% and 24.6 ± 1.2%, respectively. D-DHP407 hydrogel was biocompatible and able to support NIH-3T3 cell proliferation. Furthermore, D-DHP407 hydrogel showed intrinsic antifungal and antibacterial activity against *C. albicans* and Gram-positive *S. aureus* and Gram-negative *E. coli* bacteria, injectability and capability to retain shape post-injection, making it promising for future use in the management of hard-to-close skin wounds.

1. Introduction

Chronic skin wounds represent one of the leading concerns faced by healthcare systems daily, as millions of patients suffer from this pathology worldwide. The treatment of hard-to-close wounds is a huge economical burden requiring expensive medical cares, long hospitalization and often leading to unsuccessful tissue healing. The major cause of delayed or failed wound closure is the spreading of high level of bacteria in the wound site, which promote the biofilm formation and interfere with the common pathways of matrix metalloproteinases responsible for tissue regeneration [1]. Indeed, at least 60% of chronic wounds are associated with bacteria contamination and biofilm formation [2,3]. Thus, to promptly tackle infections and disrupt the biofilm, patients affected by chronic wounds are generally treated with high dosages of systemically- or topically-administered antibiotics [4,5]. However, in recent years this strategy was reported to be disastrous in many cases as wounds are generally invaded by strong antibiotic-resistant bacteria as a consequence of the excessive and indiscriminate use of antibiotics [6]. For these reasons, researchers are hardly working on alternative antibiotic-free strategies to manage hard-to-close infected wounds. Among them, the topical administration of antimicrobial therapeutic agents has gained increasing interest. For instance, the release of silver nanoparticles directly in the wound bed from delivery systems engineered in different forms, such as gel-membrane [7], electrospun meshes [8] and sponges [9], has been widely studied. A similar approach was also explored for the release of iron oxide [10], titanium dioxide [11] and zinc oxide [12] nanopar-

* Corresponding author.
E-mail address: monica.boffito@polito.it (M. Boffito).

https://doi.org/10.1016/j.engreg.2021.12.001
Received 29 October 2021; Received in revised form 3 December 2021; Accepted 3 December 2021
Available online 7 January 2022

ticles. An alternative approach was also explored through the design of formulations able to release naturally-derived antimicrobial agents, such as tannic acid [13], gallic acid [14] and curcumin [15]. However, such systems suffer from poor stability of the antimicrobial agent, thus resulting in a narrow therapeutic window. Furthermore, the main purpose of such systems is strictly related to their antimicrobial behavior, while no evidences have been reported on their regeneration capability. More recently, researchers have been focusing their attention on the development of synthetic antimicrobial peptides due to their remarkable capability to concurrently face infections and promote wound closure [16]. Compared to antibiotic-based treatments, the above-mentioned strategies show the advantage not to induce bacteria resistance and to exhibit a much broader spectrum of activity [17]. However, to avoid cytotoxic effects on mammalian cells, very low dosages of such antimicrobial agents can be administered, thus reducing their antimicrobial potentialities [18]. Moreover, they are generally characterized by a short-term antimicrobial activity [18]. On the other hand, concerning synthetic antimicrobial peptides, their use is limited by their cost and very fast degradation phenomena when in contact with the hostile environment (e.g., exudate alkalinity) of infected wounds. Hence, the development of more effective, cytocompatible and low-cost wound dressings able to face wound infections and promote tissue healing is an urgent need. In this scenario, the development of antimicrobial polymers represents a promising alternative to successfully face wide-spectrum bacteria contamination as widely reviewed by several research groups [18–20]. Specifically, a critical analysis of this literature highlighted the importance to make antimicrobial polymers fulfill proper requirements to provide them with antimicrobial features. More in detail, such requirements concern the average molecular weight (between 50 and 120 kDa), the hydrophobic/hydrophilic balance, the presence of positively charged functional groups and the degree of polymerization [21–23]. In this context, polyurethane (PU) chemistry represents a powerful tool, giving the possibility to synthesize high molecular weight polymers with desired properties by selecting the starting building blocks. For instance, by selecting a peptide sequence containing the Ala-Ala motif as chain extender, Silvestri et al. developed PUs with sensitivity to elastase-mediated hydrolysis [24]; Kim and colleagues synthesized a pH-responsive PU by chain extending the prepolymer with 1,4-bis-(2-hydroxyethyl)piperazine [25], while Hsiao and co-workers selected 2-hydroxyethyl methacrylate as end-capping molecule to introduce PU responsiveness to light irradiation [26]. In this work, the wide versatility of PU chemistry was explored to design an amphiphilic high molecular weight poly(ether urethane) (PEU) with antimicrobial properties to develop an injectable drug delivery carrier able to concurrently reduce infections and release therapeutic agents. More in detail, the amphiphilic triblock copolymer Poloxamer® 407 and a diol bearing a Boc-protected secondary amino group (i.e., N-Boc diethanolamine) were selected as macrodiol and chain extender, respectively, to ensure PEU amphiphilic nature and the exposure of cationic moieties along its chains. Considering the crucial role exerted by polymer amphiphilicity, molecular weight and cationic functional groups in their intrinsic antimicrobial properties, great attention was paid to the polymerization reaction to maximize the chain extension step and thus, the exposure of secondary amino groups per chain. Moreover, the presence of hydrophobic/hydrophilic blocks was investigated both at the nano- and macro-scale to design thermosensitive micellar hydrogels able to undergo sol-to-gel transition at physiological temperature. Furthermore, hydrogel potential exploitation as mini-invasive and multi-functional carrier in the treatment of hard-to-close skin wounds was investigated through the *in vitro* release of Bovine Serum Albumin (BSA) as model protein and by testing its injectability in physiological-mimicking conditions. Lastly, the biocompatibility as well as the antimicrobial activity of the designed PEU-based vehicle was evaluated through *in vitro* cytocompatibility tests according to the ISO 10993-5 regulation and through antimicrobial tests against different bacteria and fungi present in both the early and late stage of wound infection.

2. Materials and methods

2.1. Materials

Poloxamer® 407 (P407, poly(ethylene oxide)-poly(propylene oxide)-poly(ethylene oxide) triblock copolymer, $\bar{M}_n$ 12,600 Da, 70% w/w poly(ethylene oxide)), N-Boc diethanolamine, 1,6-hexamethylene diisocyanate (HDI) and dibutyltin dilaurate (DBTDL) were purchased from Sigma Aldrich, Italy. Before use, reagents were treated to remove residual water content according to the procedure reported by Laurano and Boffito [27]. All solvents were purchased from Carlo Erba Reagents (Italy) in analytical grade.

2.2. Poly(ether urethane) synthesis

The P407-based poly(ether urethane) was synthesized under nitrogen atmosphere following a two-step procedure as previously described for similar PEUs [28,29]. However, to obtain a stoichiometrically correct pre-polymer and consequently, to maximize the chain extension step and the number of –NH groups/chain, both the first and second step of PEU synthesis were optimized in terms of macrodiol concentration and reaction time as thoroughly described in paragraph 2.2.1 and 2.2.2, respectively.

2.2.1. Optimization of the pre-polymerization step

P407 was first solubilized in anhydrous 1,2-dichloroethane (DCE) at 10 and 20% w/V concentration and equilibrated at 80 °C before the addition of HDI at 2:1 molar ratio with respect to P407. The first step of the synthesis started with the addition of a catalytic amount of DBTDL (0.1% w/w concentration with respect to the macrodiol). To evaluate the pre-polymerization reaction kinetics, 2 mL of pre-polymer solution were taken from the mixture at predefined time points, i.e., 30 min, 60 min, 90 min, 120 min and 150 min, and anhydrous methanol (MeOH, Sigma Aldrich, Italy) was added to passivate isocyanate terminal groups. Subsequently, the pre-polymer was collected by precipitation in petroleum ether (4:1 volume ratio with respect to DCE reaction volume) and chromatografically analyzed according to the protocol reported below.

Hereafter, the prepolymer will be referred to as HP407_X%_Ymin, where H and P407 identify the diisocyanate and the macrodiol, respectively, whereas X and Y stand for P407 concentration and reaction time, respectively.

2.2.2. Optimization of the chain extension step

To investigate the chain extension reaction kinetics, P407 was first dissolved in DCE at the most promising concentration, resulting from the first step optimization and equilibrated at 80 °C. Then, HDI (2:1 molar ratio with respect to P407) and DBTDL (0.1% w/w concentration with respect to P407) were added to the mixture and the reaction proceeded for the previously defined time interval. At the end of the first step, the reaction volume was quickly equilibrated at 60 °C before the addition of N-Boc diethanolamine (5% w/V in DCE) at 1:1 molar ratio with respect to P407. Subsequently, the chain extension reaction was carried on for predefined time intervals, i.e., 1, 2, 3, 5 and 20 h. At each time point, 2 mL of polymer solution were taken from the mixture, MeOH was added to stop the reaction, and the PEU was collected through precipitation (in petroleum ether at 4:1 volume ratio with respect to DCE reaction volume). The polymer was then purified through precipitation in a diethyl ether/MeOH mixture (polymer solubilized at 20% w/V, diethyl ether/MeOH at 98:2 V/V and 5:1 volume ratio with respect to DCE), collected by centrifugation (6,000 rpm, 0 °C, 20 min, MIKRO 220R, Hettich, Germany) and finally chromatografically analyzed after drying.

Hereafter, the PEU will be referred to with the acronym DHP407_Yh, where D, H and P407 indicate the chain extender, the diisocyanate and the macrodiol, respectively, while Y stands for the reaction time.

2.3. Poly(ether urethane) chemical characterization

2.3.1. Size exclusion chromatography

To investigate synthesis reaction kinetics and to define the optimal parameters giving a low molecular weight pre-polymer and a high molecular weight chain-extended polymer, Size Exclusion Chromatography (SEC) analyses were performed on both HP407_X%_Ymin and DHP407_Yh through an Agilent Technologies 1200 Series (CA, USA). The instrument was equipped with a Refractive Index (RI) detector and two Waters Styragel columns (HR1 and HR4) conditioned at 55 °C. N,N-dimethylformammide (DMF, CHROMASOLV Plus, inhibitor free, for HPLC, 99.9%, Carlo Erba Reagents, Italy), added with 0.1% w/V LiBr (Sigma Aldrich, Italy), was used as mobile phase. A calibration curve based on poly(ethylene glycol) standards was defined in the range of peak molecular weight M_P 4,000–200,000 Da. Before analyses, 2 mg of polymer were dissolved in 1 mL of mobile phase and filtered through a 0.45 μm syringe filter (poly(tetrafluoroethylene) membrane, Whatman). Number Average Molecular Weight ($\bar{M}_n$), Weight Average Molecular Weight ($\bar{M}_w$) and polydispersity index (D) were estimated using the Agilent ChemStation software. Analyses were performed on all the collected aliquots and results are reported as molecular weight distribution profiles and $\bar{M}_n$, $\bar{M}_w$ and D values.

2.3.2 Attenuated total reflectance Fourier transform infrared spectroscopy

Attenuated Total Reflectance Fourier Transform Infrared (ATR-FTIR) spectroscopy was conducted on all HP407_X%_Ymin and DHP407_Yh samples to verify the appearance and intensity growth of the characteristic urethane bands. Analyses were performed at room temperature (RT) using a Perkin Elmer Spectrum 100 (PerkinElmer, MA, USA) equipped with an ATR accessory (UATR KRSS) with diamond crystal. Spectra resulted from 32 scans in the range 4,000–600 cm^{-1} with a resolution of 4 cm^{-1}. Data were elaborated using the Perkin Elmer software.

2.4. Secondary amino group exposure

To remove Boc protecting groups, thus exposing the secondary amino groups present along PEU backbone, all DHP407_Yh aliquots were subjected to an acidic treatment according to the procedure recently published by Laurano et al. [30]. Briefly, for each sample, 1 g of polymeric powders were first dissolved in 22.5 mL of chloroform for 2 h, at RT, under magnetic stirring (250 rpm) and continuous nitrogen flow. Afterwards, 2.5 mL of trifluoroacetic acid (TFA, Sigma Aldrich, Italy) were added and Boc cleavage reaction was carried on at RT for 1 h. Next, to remove both chloroform and TFA the deprotected polymer solution was first concentrated in a rotary evaporator (Buchi Rotavapor Labortechnik AG, Switzerland), washed twice with 10 mL of chloroform and lastly, dissolved in 20 mL of double distilled water (ddH_2O) under vigorous stirring at 4 °C overnight. Finally, the deprotected PEU solution was dialyzed (10–12 kDa cut-off membrane, Sigma Aldrich, Italy) for 48 h against ddH_2O to wash Boc groups and residual solvent traces out and freeze-dried using a Martin Christ ALPHA 2-4 LSC (Germany) instrument.

Hereafter, PEU exposing free –NH groups will be referred to as D-DHP407_Yh, where the acronym D-DHP407 identifies DHP407 PEU subjected to Boc deprotection reaction and Y stands for the duration of the chain extension reaction.

2.5. Characterization of the poly(ether urethane) exposing amino groups

2.5.1. Size exclusion chromatography

In order to investigate whether the deprotection reaction could affect the integrity of PEU bonds, SEC analyses were performed according to the previously described protocol. Specifically, all D-DHP407_Yh were analyzed and results compared to the corresponding control (i.e., DHP407_Yh).

2.5.2. Attenuated total reflectance Fourier transform infrared spectroscopy

ATR-FTIR analyses were performed on all D-DHP407_Yh according to the previously described protocol to assess the presence of the characteristic urethane bonds after the acidic treatment carried out to expose secondary amino groups.

2.5.3. Orange II sodium salt colorimetric assay

Secondary amino groups exposed along D-DHP407_Yh polymer backbone were quantified through a colorimetric assay (Orange II Sodium Salt, Sigma Aldrich, Italy) according to the method proposed by Laurano et al. [30]. Briefly, a 0.5 mM Orange II Sodium Salt solution was first prepared in ddH_2O and the pH was adjusted to 3 with HCl 1 M. Subsequently, 20 mg of D-DHP407_Yh samples were solubilized in 50 mL of the dye solution and the electrostatic coupling reaction between the cationic D-DHP407_Yh and the anionic Orange molecules was carried on for 18 h, at RT and in the dark. Then, samples were put in dialysis (10–12 kDa cut-off membrane, Sigma Aldrich, Italy) against ddH_2O for 72 h to remove the unreacted dye and lastly, freeze-dried using a Martin Christ ALPHA 2-4 LSC (Germany) instrument. Control samples (DHP407_Yh) were also subjected to the same procedure to evaluate the amount of absorbed dye. Lastly, lyophilized samples were solubilized at 10 mg/mL in ddH_2O adjusted to pH 12 with NaOH 1 M to desorb grafted/absorbed Orange molecules. The incubation was carried on in the dark at RT for 2 h and then, samples were centrifuged at 15 °C, 6,000 rpm for 10 min to separate the polymer. Extract absorbance was measured at 485 nm using an UV-Vis spectrophotometer (PerkinElmer, Lambda 25, MA, USA) and –NH groups were finally quantified referring to a calibration curve based on Orange molecules dissolved at predefined concentrations (range: 5–83.4 μM) in ddH_2O at pH 12. The colorimetric assay was performed in triplicate and results are reported as mean ± standard deviation.

2.5.4. Critical micelle concentration

The Critical Micelle Concentration was estimated for the D-DHP407_Yh polymer exposing the highest number of secondary amines and the corresponding DHP407_Yh PEU. Solutions of both poly(ether urethane)s at 0.8 mg/mL were prepared by dissolving the polymers in alkaline deionized water. The Critical Micelle Concentration (CMC) was obtained by measuring the surface tension of serially diluted PEU solutions prepared (range: 0.8 mg/mL - 0.0005 mg/mL) in alkaline deionized water. P407 macrodiol was tested according to the same procedure as control condition, being the PEU component driving the micellar organization. The measurements were carried out at 25 °C with a ring tensiometer (Sigma 703D, KSV INSTRUMENTS LTD, Finland) according to the Du-Nouy ring method. Surface tension of each dilution was determined in triplicate and data were expressed as mN/m. The value of CMC was defined as the intersection point of the straight lines extrapolated from the concentration-dependent and concentration-independent sections of the curve obtained by plotting the compound concentration *vs.* the corresponding surface tension [31].

2.6. Characterization of poly(ether urethane) thermosensitivity

To investigate whether the exposure of secondary amino groups could affect the characteristic temperature-driven PEU chain capability to arrange into micelles and to undergo physical gelation upon dissolution in an aqueous medium, micelle average diameter, Critical Micellar Temperature and sol-to-gel transition potential were thoroughly studied. Samples were prepared starting from the deprotected PEU exposing the highest number of -NH groups (hereafter referred to with the acronym D-DHP407) as assessed by Orange II Sodium Salt assay. The corresponding Boc-protected DHP407 PEU was tested according to the same protocols as control condition.

2.6.1. Dynamic light scattering

Dynamic Light Scattering (DLS) measurements were performed on both DHP407 and D-DHP407 solutions prepared in physiological saline

solution (0.9% w/V NaCl) at 1% w/V polymeric concentration. Analyses were performed at 25, 30 and 37 °C, according to the protocol reported by Laurano et al. [30], using a Zetasizer Nano S90 (Malvern Instruments, Worcestershire, UK) instrument. Before starting, samples were equilibrated at the test temperature for 15 min and then analyzed according to Pradal et al. [32]. The reported hydrodynamic diameters resulted from the average of three different analyzed samples. Data are reported as mean ± standard deviation.

2.6.2. Critical Micellar temperature evaluation

The Critical Micellar Temperature (CMT) of DHP407 and D-DHP407-based solutions was estimated using a fluorescent dye (1,6-diphenyl-1,3,5-hexatriene, DPH, Sigma Aldrich, Italy) as micellization marker. Polymers were first solubilized at 1 mg/mL in physiological saline solution (0.9% w/V NaCl) and then, 10 μL/mL of DPH solution (previously dissolved in methanol at 0.4 mM) was added to each sample. Analyses were conducted according to the method described by Alexandridis et al. [33]. Briefly, PEU solutions were heated between 5 and 40 °C at 1 °C/step, each step consisting of 5 min temperature equilibration followed by UV/Vis spectra recording in the 500–300 nm spectral range (PerkinElmer, Lambda 25, MA, USA). CMT values were defined as the first inflection of the sigmoidal curve obtained by plotting the absorbance intensity at 356 nm *vs.* temperature as described by Boffito et al. [34]. Analyses were performed in triplicate and results are reported as mean ± standard deviation.

2.6.3. Tube inverting test in isothermal and temperature-ramp conditions

Tube Inverting Test was exploited to qualitatively determine the Critical Gelation Concentration (CGC) and to evaluate the sol-to-gel transition temperature and kinetics of polymeric aqueous solutions prepared starting from DHP407 and D-DHP407 PEUs. To this purpose, 1 mL of polymeric solutions were prepared in bijou sample container with an inner diameter of 17 mm (Carlo Erba Reagents, Italy) by dissolving the polymeric component (range: 5–25% w/V) in physiological saline solution. Analyses were performed in both temperature ramp (range: 5–70 °C, 1 ± 0.1 °C/step within 30 s) and isothermal (i.e., 37 °C) conditions. In the former test, samples were incubated for 5 min at the selected temperature and then, the vials were inverted to visually inspect the sol-to-gel transition. In the latter test, samples were kept continuously at 37 °C and inverted after each minute for 30 s in the range 1–10 min. Sol and gel conditions were defined as reported by Laurano and Boffito et al. [35]. Briefly, the presence and the absence of flow along the vial wall within 30 s of inversion were defined as the sol and gel state, respectively.

2.6.4. Rheological characterization

To thoroughly investigate hydrogel thermo-responsiveness, PEU-based gelling solutions were rheologically characterized using a stress-controlled rheometer (MCR302, Anton Paar Gmbh, Graz, Austria). The instrument was equipped with a 50 mm parallel plate geometry and a Peltier system for temperature control. Samples were prepared in physiological saline solution by dissolving the polymer at the optimal concentration in terms of gelation conditions as defined by the previously described qualitative tests. Then, formulations were analyzed through: temperature ramp tests (0–40 °C, 2 °C/min, 0.1 s^{-1} frequency) to study the sol-to-gel transition; strain sweep tests (10 Hz, strain range 0.01–500%, 37 °C) to investigate gel resistance to applied deformation at physiological temperature and lastly, frequency sweep tests (frequency range 0.1–100 rad/s, strain 0.1% at 25, 30 and 37 °C) to characterize gel viscoelastic properties at different temperatures. For each analysis the sample was poured on the lower plate of the instrument in the sol state at 0 °C, heated at the test temperature and equilibrated for 10 min to reach thermal stability, and finally tested.

2.7. Bovine Serum Albumin release study

To investigate hydrogel potentialities as drug/biomolecule delivery system in the treatment of hard-to-close skin wounds, the release of Bovine Serum Albumin (BSA, Sigma Aldrich, Italy) as model protein was evaluated from both DHP407 and D-DHP407 formulations. Specifically, BSA was first solubilized at 1 mg/mL in physiological saline solution; then, this solution was used to dissolve both polymers at the optimized concentration (as defined from previous characterizations) at 4 °C overnight. Subsequently, samples (0.8 mL) were equilibrated at 37 °C for 15 min to allow a complete sol-to-gel transition and then 0.8 mL of Phosphate Buffered Saline solution (PBS, pH 7.4, Sigma Aldrich, Italy, previously equilibrated at 37 °C) were added to each gel as releasing medium. At predefined time points (i.e., 2 h, 4 h, 6 h, 1 d, 2 d, 3 d, 4 d and 7 d) the medium was collected and 0.8 mL of fresh PBS were added upon each sample. The amount of released BSA was then quantified by using the colorimetric QuantiPro™ BCA assay kit (Sigma Aldrich, Italy) and by referring to a BSA calibration curve (protein concentration ranging between 1 μg/mL and 10 μg/mL). Briefly, 150 μL of each extract were mixed with an equal volume of BCA working solution prepared according to the manufacturer's protocol. Then, the samples were incubated at 60 °C for 1 h and lastly, the absorbance at 562 nm was measured through a multimode plate reader (VICTOR X3, Perkin Elmer, MA, USA). Analyses were performed in triplicate and results are reported as average values ± standard deviation.

2.8. Evaluation of hydrogel injectability

In the perspective of hydrogel application as mini-invasive drug/biomolecule delivery carrier, system injectability was evaluated through needles of different size by three independent operators. Specifically, both DHP407 and D-DHP407 formulations were first prepared in physiological saline solution at the optimized concentration as defined from previous characterizations. Then, they were loaded in 3 mL plastic syringes (Carlo Erba Reagents, Italy) and equilibrated at 4, 25 and 37 °C for 30 min. Lastly, hydrogel injectability was evaluated through G22, G21, G18 and G16 needles.

Furthermore, by using a G18 needle, PEU formulations were also tested to qualitatively investigate hydrogel capability to be injected in the sol state and to undergo fast sol-to-gel transition at physiological temperature, thus avoiding material flow. To this purpose, a hole was first performed on an apple surface previously equilibrated at 37 °C; then, the formulation was injected to cover the entire surface and lastly, the apple was incubated for 5 min at 37 °C before visual inspection. On the other hand, to simulate tissue resistance during injection the same formulation was also injected through a G18 needle in a piece of chicken meet previously equilibrated at physiological temperature.

2.9. In vitro poly(ether urethane) biocompatibility

To assess hydrogel biocompatibility, cell cytotoxicity/viability tests were conducted through a multiplex assay on both DHP407 and D-DHP407 extracts using NIH-3T3 murine fibroblasts (ATCC® CRL-1658, ATCC®, USA). NIH-3T3 cells were regularly cultured in complete medium composed of Dulbecco Modified Eagle's Medium (DMEM, ATCC®, USA) added with Mycozap PLUS antibiotic (Lonza, Switzerland), according to the manufacturer's instruction, and 10% V/V Bovine Calf Serum (BCS, ATCC®, USA) and incubated in a humidified incubator at 37 °C, 5% CO_2. Before the experiments, cell supernatant was tested for mycoplasma by using the MycoAlert Plus Mycoplasma Detection kit (Lonza, Switzerland) to assess the absence of contaminations.

2.9.1. Preparation of hydrogel extracts

Hydrogel extracts were prepared according to the ISO 10993-5 regulation. Briefly, DHP407 and D-DHP407 polymers were first dissolved

in physiological saline solution at the optimized concentration (as defined from previous characterizations) at 4 °C overnight. Then, 250 μL of gelling solution were poured in the sol state in a 24-well plate and incubated for 10 min at 37 °C to allow a complete sol-to-gel transition. Subsequently, 2.5 mL of pre-heated complete medium were added upon each gel and incubated at 37 °C for 24 h. Finally, extracts were collected and filtered through a 0.22 μm syringe filter (Poly(ether sulfone) membrane, Carlo Erba Reagents, Italy) under a sterile hood.

2.9.2. Cell cytotoxicity evaluation

Cell cytotoxicity was evaluated using CytoTox-ONE™ homogeneous membrane integrity assay (Promega). Cells were first seeded in a sterile 96-well plate at 10,000 cells/well and incubated at 37 °C, 5% CO_2 for 24 h to allow cell adherence. Then, the complete medium was removed, 100 μL of hydrogel extracts were added in each well and the plate was again incubated at 37 °C, 5% CO_2 for 24 h. Afterwards, cell cytotoxicity was evaluated according to the manufacturer's instruction. Briefly, 100 μL of CytoTox-ONE Reagent were added to each well and the plate was kept at room temperature for 10 min, followed by the addition of 50 μL of stop solution. Cells cultured in complete medium and cells lysed with a 9% Triton® X-100 (Promega) were used as negative and positive controls, respectively. Lastly, the fluorescence was quantified through a multimode plate reader (VICTOR X3, Perkin Elmer, MA, USA) at Ex/Em 535/590 nm and cell cytotoxicity was calculated as percentage by referring to the positive control. Analyses were performed in triplicate and results reported as average values ± standard deviation.

2.9.3. Cell viability evaluation

Cell viability was evaluated using the CellTiter-Blue® cell viability assay (Promega,USA). Cells were first seeded at 10,000 cells/well and cultured for 24 h as previously described for cytotoxicity tests. Then, the complete medium was removed, replaced with 100 μL of hydrogel extracts and lastly, the 96-well plate was incubated at 37 °C, 5% CO_2 for 24 h. Subsequently, cell viability was evaluated according to the manufacturer's instructions. Briefly, 20 μL of CellTiter-Blue® solution were added to each well and the plate was incubated again in normal culture conditions for 3 h. Cells cultured in complete medium and cells lysed with a 9% Triton® X-100 (Promega, USA) were used as negative and positive controls, respectively. Lastly, the fluorescence was quantified through a multimode plate reader (Victor X3, Perkin Elmer, MA, USA) at Ex/Em 535/590 nm and cell cytotoxicity was calculated as percentage by referring to the negative control. Analyses were performed in triplicate and results reported as average values ± standard deviation.

2.9.4. Cell proliferation

Cell proliferation was evaluated using the CytoTox-ONE™ homogeneous membrane integrity assay (Promega, USA). Specifically, cells were first seeded in a 96-well plate at 10,000 cells/well and cultured for 24 h to allow adherence (t0); then, the complete medium was removed, replaced with 100 μL of hydrogel extracts and the plates were incubated in normal culture conditions for 24, 48 and 72 h. Cells cultured in complete DMEM were used as negative control. At each time point cells were lysed with a 9% Triton® X-100 (Promega, USA) and the CytoTox-ONE™ assay was performed as previously described. Lastly, cell proliferation was calculated by referring to the fluorescence value measured at t0 and results reported as average values ± standard deviation.

2.10. In vitro antibacterial activity

The susceptibility of *Staphylococcus aureus* (ATCC® 25923, ATCC®, USA), *Pseudomonas aeruginosa* (ATCC® 10145, ATCC®, USA), *Escherichia coli* (ATCC® 25922, ATCC®, USA) and *Candida albicans* (ATCC® 10231, ATCC®, USA) to both DHP407 and D-DHP407 PEUs and P407 polymer was determined in 96-well microtiter plates using the broth dilution method described in Mancuso et al. [36] and Ceresa et al. [37], with some modifications. Each polymer was tested at concentrations ranging from 0 to 25 mg/mL. Bacterial suspensions at the concentration of 5×10^5 Colony Forming Unit (CFU)/mL were prepared in Mueller-Hinton Broth (Sifin Diagnostics GmbH, Berlin, Germany). Fungal suspensions (0.5–2.5 × 10^5 CFU/mL) were prepared in RPMI-1640 (Sigma Aldrich, St. Louis, MO, United States) buffered with 3-(N-morpholino)propanesulfonic acid buffer (MOPS) (Sigma Aldrich, St. Louis, MO, United States) and supplemented with 2% D-glucose (Sharlab, Barcelona, Spain), pH 7.0. Blank wells containing medium only were also included. Plates were incubated at 37 °C for 20 h. Afterwards, absorbance at 595 and 450 nm was detected for bacterial and fungal strains (Ultramark Microplate Imaging System, Bio-Rad, USA), respectively, and percentages of growth inhibition were calculated. Experiments were performed in triplicate and repeated three times. Results were reported as average absorbance values ± standard deviation. The same polymeric concentrations were also tested for cytocompatibility after 24 h of incubations with confluent NIH-3T3 murine fibroblasts to clearly discern potential cytotoxic and antibacterial properties.

2.11. Statistical analysis

Statistical analysis was performed using GraphPad Prism 8.0 for MacOsX (GraphPad Software, La Jolla, CA, USA; www.graphpad.com). Two-way ANOVA analysis followed by Tukey's multiple comparisons test was used to compare results. The statistical significance of each comparison was assessed as follows: $p < 0.0001 = ^{****}$, $0.0001 < p < 0.001 = ^{***}$, $0.001 < p < 0.01 = ^{**}$, $0.01 < p < 0.5 = ^{*}$.

3. Results and discussion

3.1. Optimization of poly(ether urethane) synthesis and characterization of the amino group exposure procedure

The chemistry of polyurethane was here selected as a versatile tool to design injectable drug delivery systems with intrinsic antimicrobial features. Indeed, polyurethane chemistry allows the preparation of polymers with target properties depending on reacting building blocks. Polymer requirements for antimicrobial activity include amphiphilicity, exposure of cationic groups [18–20] and high molecular weight (M_w = 50–120 kDa). Based on that, Poloxamer® 407 and N-Boc diethanolamine were selected as amphiphilic macrodiol and –NH containing chain extender, respectively and the synthesis reaction was controlled to obtain high molecular weight PEUs. Synthesis reaction was optimized in terms of macrodiol concentration and reaction time to obtain polymers with macrodiol/diisocyanate/chain extender 1:2:1 molar ratio (Fig. S1) and characterized by molecular weights comparable to the expected theoretical values. Subsequently, aiming at collecting further insight on the chain extension reaction and undoubtedly define the optimal reaction time for the chain extension step, exposed -NH groups were quantified on DHP407_Yh samples upon an acid treatment to remove the Boc-caging groups [30]. More in detail, deprotected PEUs (D-DHP407_Yh) were first characterized through ATR-FTIR spectroscopy and SEC analyses to verify the integrity of the urethane bonds after the acidic treatment; then, secondary amino groups were quantified through the colorimetric Orange II Sodium Salt assay. Lastly, the Critical Micellar Concentration was evaluated for both DHP407 and D-DHP407 formulations to investigate whether the removal of Boc caging groups, and thus the exposure of secondary amino groups, could affect the minimal polymeric concentration that allows chain arrangement into micelles.

3.1.1. Optimization of the pre-polymerization step

To synthesize a pre-polymer with close molecular weight to the theoretical value (achieved at macrodiol:diisocyanate 1:2 molar ratio), the influence of macrodiol concentration (10 and 20% w/V) and reaction time (30, 60, 90, 120, 150 min) on pre-polymer molecular weight was

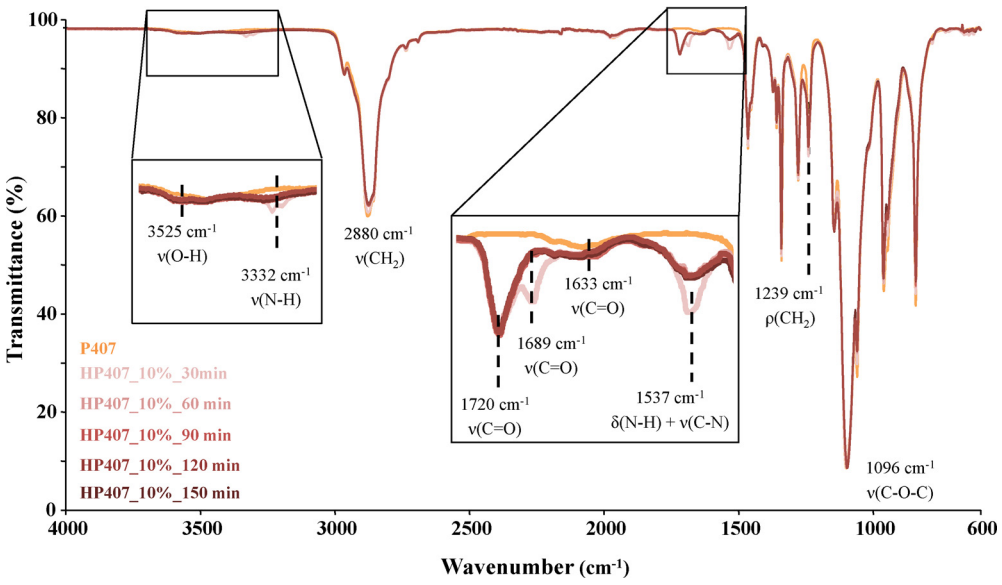

Fig. 1. ATR-FTIR spectra of P407 (orange spectrum) and HP407_10%_Ymin: curves from light red to dark red indicate ATR-FTIR spectra of pre-polymers obtained at increasing reaction time from 30 to 150 min. The boxes highlight the wavenumber regions with the more marked differences among the spectra.

investigated. ATR-FTIR spectroscopic analyses were first performed on both HP407_10%_Ymin and HP407_20%_Ymin (Figs. 1 and S2).

Irrespective of reaction conditions, the spectra showed the characteristic absorption peaks of P407 bonds at: 1,096, 2,280 and 1,239 cm^{-1} ascribed to C-O-C stretching vibrations and to CH_2 stretching and rocking vibrations, respectively. ATR-FTIR spectra confirmed the formation of urethane bonds with bands at 1,720 and 1,630 cm^{-1} (stretching vibration of carbonyl groups), 1,537 cm^{-1} (N-H bending and C-N stretching vibrations) and 3,332 cm^{-1} (N-H stretching vibration) [38]. Moreover, the band at 1,630 cm^{-1} can also be attributed to the stretching vibration of the carbonyl groups belonged to urea bonds. Indeed, reactions carried out at high temperature (i.e., higher than 65 °C) in the presence of DBTDL as catalyst and/or residual water coming from reagents and/or solvents may lead to urea by-products, as previously reported [28,39]. Nevertheless, ATR-FTIR characterization confirmed the successful synthesis of pre-polymers. However, no time-dependent differences were observed between HP407_10%_Ymin and HP407_20%_Ymin spectra, suggesting that ATR-FTIR analysis cannot provide information on reaction kinetics. Indeed, the growing number of urethane bonds during reaction progression was not detectable by ATR-FTIR spectroscopy. However, both HP407_10%_30 min and HP407_20%_30 min showed the appearance of a new peak in the region of carbonyl groups stretching (i.e., at 1,689 cm^{-1}) and higher intensity peaks at 1,537 and 3,332 cm^{-1} ascribed to the –NH bond vibrations. These differences can be probably attributed to intermediate compounds as they could not be detected after 60 min of reaction.

Interestingly, SEC analyses showed increasing trends in Number Average Molecular Weight ($\bar{M}_n$) and Weight Average Molecular Weight ($\bar{M}_w$) for both HP407_10%_Ymin and HP407_20%_Ymin as a function of reaction time (Fig. 2_A and B). Irrespective of P407 initial concentration, both $\bar{M}_n$ and $\bar{M}_w$ increased by increasing reaction time up to 120 min. However, further reaction time increase up to 150 min did not cause the formation of polymers with higher molecular weight, probably due to the achievement of equilibrium condition between reagents and product concentrations. On the other hand, at the same reaction time, HP407_20% showed slightly higher molecular weights compared to HP407_10% up to 60 min reaction time, suggesting that macrodiol concentration had a positive influence on reaction kinetics. A higher P407 concentration may favor interactions between the macrodiol and the diisocyanate molecules, leading to quicker formation of urethane bonds at the same reaction time.

Concerning molecular weight distribution, extremely different profiles could be observed between HP407_10%_Ymin and HP407_20%_Ymin (Fig. 2_C and D, respectively) especially for short reaction times (i.e., up to 90 min). Specifically, three main peaks could be identified up to 90 min of reaction in HP407_10%_Ymin at 6,000, 14,000 and 26,000 Da, ascribable to P407 diblocks as recently reported by Laurano et al. [40], P407 triblocks and higher molecular weight chains, respectively. With further increasing reaction time, the peaks attributed to the macrodiol tended to decrease in intensity, suggesting the progressive consumption of this reagent. On the other hand, the peak attributed to higher molecular weight components tended to become broader with increasing reaction time. These observations suggested the formation of an increasing number of high molecular weight chains as a function of reaction time, rather than an increased concentration of isocyanate-terminated pre-polymers with molecular weight of approx. 13,000 Da. Therefore, the estimated high average molecular weights for long reaction times resulted from the formation of a considerable amount of not-stoichiometric pre-polymers. This consideration was further supported by the increasing polydispersity index from 1.3 at 30 min reaction time to 1.8 at 150 min reaction time.

On the other hand, considering the SEC profiles obtained from HP407_20%_Ymin (Fig. 2_D), the three peaks at 6,000, 14,000 and 26,000 Da could be slightly identified only at 30 min of reaction. Indeed, from 60 min up to 150 min a broadening of the M_i distribution profile was observed, which suggested the progressive formation of pre-polymers characterized by higher molecular weights than the theoretical expected value (i.e., approx. 13 kDa). A further confirmation was obtained by the measured polydispersity indexes, which increased from 1.6 at 30 min reaction time up to 1.8 at 150 min of chain extension.

Although not statistically significant differences were observed in terms of average molecular weights by comparing HP407_10% and HP407_20% at the same reaction time, the molecular weight distributions were different. Specifically, HP407_20% showed an important high molecular weight component already at 30 min of reaction. On the other hand, HP407_10% exhibited a small contribution of the high molecular weight component up to 60 min of reaction: at low macrodiol concentration of 10% w/V and short reaction times (i.e., 30 and 60 min), the amount of still unreacted P407 in the mixture was considerable.

Therefore, based on these evidences, we investigated the possibility to adopt average values of both P407 concentration and reaction time, i.e., 15% w/V concentration and 45 min reaction time (Fig. S3). By selecting these reaction parameters, the SEC profile of HP407_15%_45 min showed the previously described three main peaks and, at the same time, a low contribution of the high molecular weight components ($D = 1.4$). Furthermore, the low intensity of the peak ascribed to the macrodiol suggested an almost complete reaction between the macrodiol and the diisocyanate towards the pre-polymer formation. In addition, $\bar{M}_n$ and

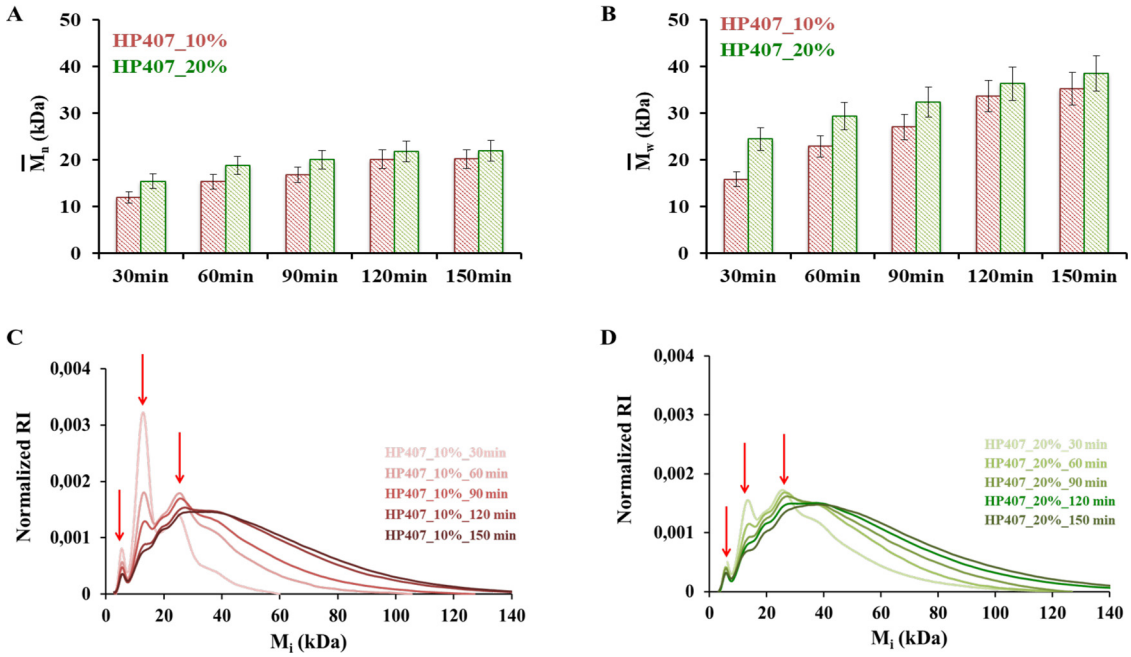

Fig. 2. Number Average Molecular Weight ($\bar{M}_n$) (A) and Weight Average Molecular Weight ($\bar{M}_w$) (B) of HP407_X%_Ymin pre-polymers formed by reacting Poloxamer® 407 with 1,6-hexamethylene diisocyanate. The red and green bars refer to P407 dissolved in anhydrous 1,2-dichloroethane at 10% and 20% w/V concentrations, respectively. Instrument error was up to 10% according to Trathnigg et al. [41]. Molecular weight distribution profiles of HP407_10%_Ymin (C) and HP407_20%_Ymin (D) obtained by plotting normalized refractive index (RI) signal *vs.* molecular weight of components (M_i) at different reaction times. The red arrows mark the peaks at 6,000, 14,000 and 26,000 Da.

Table 1
Number Average Molecular Weight ($\bar{M}_n$), Weight Average Molecular Weight ($\bar{M}_w$) and Polydispersity index (D) of DHP407_Yh samples resulting from the chain extension of HP407_15%_45 min pre-polymer with N-Boc diethanolamine for different time intervals. Instrument error up to 10% according to Trathnigg et al. [41].

	$\bar{M}_n$(Da)	$\bar{M}_w$(Da)	D
DHP407_1h	21,720	33,340	1.4
DHP407_2h	20,050	32,940	1.6
DHP407_3h	18,200	32,930	1.8
DHP407_5h	21,930	34,770	1.8
DHP407_20h	7,720	15,720	2.0

$\bar{M}_w$ were estimated to be 17,700 Da and 25,600 Da, respectively, values that are close to the theoretical pre-polymer molecular weight (i.e., $\bar{M}_n$=13,000 Da). Therefore, these reaction conditions (i.e., 15% P407 concentration and 45 min reaction time) were selected as optimal for the synthesis of pre-polymers composed by macrodiols and diisocyanates in a 1:2 molar ratio. Such reaction conditions were selected for the investigation of the second reaction step for polyurethane synthesis.

3.1.2. Optimization of the chain extension reaction step

Polymer molecular weight and density of lateral cationic groups play a key role in polymer antibacterial activity [18–20]. For this reason, the second step of PEU synthesis was optimized with the aim to maximize chain extension reaction, forming a high molecular weight polymer which exposes a high number of secondary amines (laterally exposed by the chain extender). The chain extension reaction was investigated by analyzing changes in PEU molecular weight at different reaction times. Table 1 reports $\bar{M}_n$, $\bar{M}_w$ and D values of DHP407_Yh synthesized during 1–20 h reaction of HP407_15%_45 min pre-polymer with the chain extender, while Fig. 3_A shows the molecular weight distribution profiles.

Although not significant differences were observed in $\bar{M}_w$ up to 5 h chain extension reaction, a progressive slight increase in D values was observed, suggesting a progressively wider distribution of the molecular weight. These observations were further confirmed by the analysis of molecular weight distribution profiles, showing a not negligible contribution by high molecular weight chains. However, although all DHP407_Yh samples (except for DHP407_20h) showed a similar molecular weight profile with a main peak centered at the same value (i.e., approx. 33,000 Da), its intensity slightly decreased while the intensity of the peak due to higher molecular weight components increased with increasing reaction time. On the other hand a reaction time of 20 h caused detrimental effects on average molecular weight values and molecular weight distribution profile. These findings were a consequence of a depolymerization reaction, resulting from the use of a chlorinated solvent as reaction medium (DCE), the high reaction temperature (60 °C) and the introduction of DBTDL in the reaction mixture, progressively causing the rupture of urethane bonds and/or degradation of the starting reagents.

Based on SEC analysis an optimal reaction time for the second step of PEU synthesis could not be selected as no differences were observed in polymer molecular weight profiles after 1–3 h reaction time (Fig. 3_A). However, SEC analysis suggested that 1 h reaction time represents a compromise value for the second step reaction time, ensuring efficient chain extension reaction and minimization of polymer degradation/depolymerization.

ATR-FTIR spectra (Fig. S4) confirmed the success of the reaction evidencing the formation of the characteristic urethane bonds. However, ATR-FTIR analysis did not provide information on the efficiency and extent of the chain extension reaction, as all DHP407_Yh spectra were completely overlapped. Therefore, quantification of secondary amino groups was needed to get such information.

3.1.3. Chemical characterization of the deprotected poly(ether urethane)

The comparison between DHP407_Yh and D-DHP407_Yh ATR-FTIR spectra confirmed the integrity of the urethane bonds upon Boc removal, as they were perfectly overlapped (data not reported). Therefore, the acidic treatment did not chemically alter the integrity of the PEU backbone, in accordance with previously reported works [29,30].

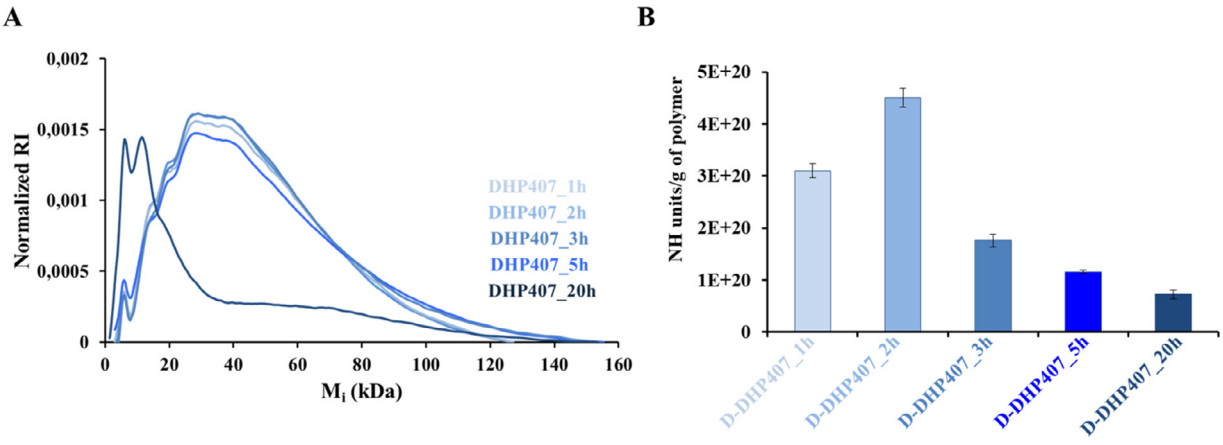

Fig. 3. Normalized Refractive Index (RI) *vs.* molecular weight of components (M_i) measured for DHP407_Yh samples obtained by chain extending HP407_15%_45 min with N-Boc diethanolamine for different time intervals (A). Secondary amino groups exposed along D-DHP407_Yh chains upon PEU acid treatment quantified through the colorimetric Orange II Sodium Salt assay (B).

Table 2
Number Average Molecular Weight ($\bar{M}_n$) estimated for DHP407_Yh and D-DHP407_Yh, i.e., after Boc removal to expose –NH groups along DHP407_Yh chains. Instrument error up to 10% according to Trathnigg et al. [41].

	$\bar{M}_n$(Da)	
	DHP407	**D-DHP407**
1h	21,720	20,500
2h	20,050	20,230
3h	18,200	18,920
5h	21,930	20,740
20h	7,720	6,980

However, no clear conclusion about the effective exposure of secondary amino groups could be achieved from ATR-FTIR spectra as only negligible differences in transmission percentage of amine-related peaks were detected.

A further confirmation of PEU integrity was obtained through SEC analyses. Indeed, considering the intrinsic error of this chromatographic technique (i.e., 10%) [41], no differences were observed in $\bar{M}_n$ values, irrespective of the considered reaction time (Table 2). Furthermore, also the molecular weight distribution profiles were almost overlapped, suggesting that the acidic treatment did not significantly alter the composition of the samples in terms of constituent molecular weight components, which overall contributed to the definition of the average values. Fig. S5 reports the molecular weight distribution profiles of DHP407_2h and D-DHP407_2h as an example.

3.1.4. Secondary amino group quantification

The quantification of secondary amino groups exposed along D-DHP407_Yh chains was carried out by adapting the colorimetric Orange II Sodium Salt assay to water-soluble polymers as described in a recently published work by Laurano et al. [30]. DHP407_Yh samples were subjected to the same protocol as control conditions to estimate color change variations ascribed to dye adsorption by PEU chains. The total number of free -NH groups exposed along D-DHP407_Yh was measured assuming that one Orange II molecule electrostatically interacts with one –NH group (Fig. 3B). As expected, the number of secondary amino groups changed as a function of chain extension reaction time. In detail, the number of functional groups increased up to 2 h reaction time, reaching $4.5 \times 10^{20} \pm 1.8 \times 10^{19}$ units/g of D-DHP407_2h. At higher reaction times, the number of functional groups decreased progressively. Therefore, although SEC analysis measured similar $\bar{M}_n$ values within the first 5 h of reaction, the corresponding degrees of chain extension were different. At long chain extension reaction time, the limited mobility of high molecular weight chains probably lowered the probability of an effective chain interaction. In addition, long reaction times could bring to a dynamic equilibrium, which results in continuous bond formation and rupture. After 20 h chain extension reaction time, the number of functional moieties was extremely lower compared to that measured in D-DHP407_2h, in agreement to SEC data. In addition, the amount of effectively deprotected –NH groups could have been overestimated, as degradation/depolymerization could occur at urethane bond sites during the reaction, particularly at long reaction times. Indeed, in the presence of residual water coming from solvents and/or reagents, urethane bond may break with the formation of carboxyl and primary amino groups, able to interact with Orange II dye during the assay.

Therefore, based on the $\bar{M}_n$ values estimated through chromatographic analyses and on the quantification of secondary amino groups through Orange II Sodium Salt assay, 2 h reaction time was selected as optimal parameter for PEU synthesis, leading to the highest chain extension degree.

Hereafter, the PEU resulting from the optimized synthesis procedure will be referred to with the acronym DHP407; consequently, D-DHP407 will stand for the deprotected DHP407. For a detailed description of the optimized protocol, refer to the supporting information file.

3.1.5. Critical micellar concentration

CMC is commonly used to measure the efficacy of surfactants, which is directly correlated to their capability to reduce the surface tension. The assay was performed on both DHP407 and D-DHP407 PEUs and on P407 macrodiol, being the building block that confers PEU amphiphilicity. Irrespective of tested polymer, a progressive decrease in surface tension was observed along with an increasing concentration. Highly active surfactants have lower CMC, which means, lower concentrations are required to decrease the surface tension. The CMC values of P407, DHP407 and D-DHP407 were calculated to be 18.9, 17.5 and 19.7 μg/mL, respectively, as shown in Fig. S6. Such differences can be attributed to chain chemical composition. More in detail, the reduction in the CMC value of DHP407 compared to P407 can be ascribed to an increased chain hydrophobic content (i.e., diisocyanate and chain extender building blocks), which favors hydrophobic interactions and chain aggregation into micelles [42]. Conversely, the increased CMC value of D-DHP407 compared to P407 can be ascribed to the strong interactions formed between –NH groups and water molecules, which consequently slightly hindered chain organization into micelles. Despite these differences, at the concentrations corresponding to CMC, all tested compounds reduced the water surface tension from 72.33 mN/m to approximately 50.9 mN/m.

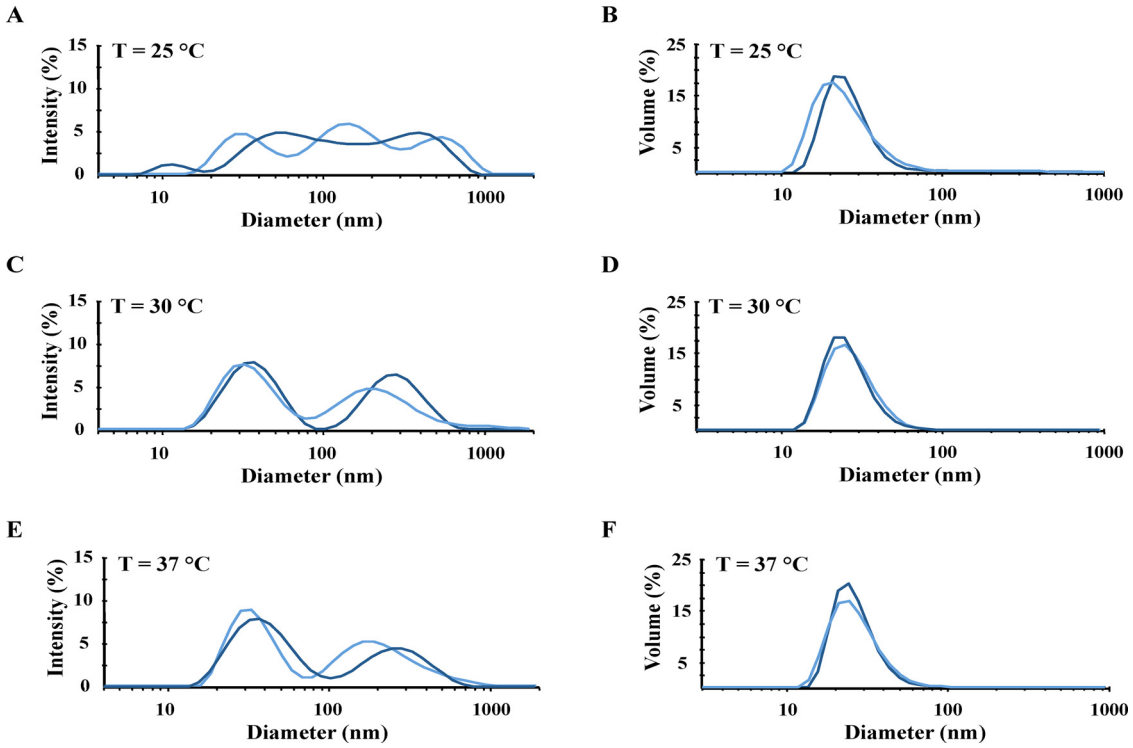

Fig. 4. Distribution patterns by intensity (A, C, E) and by volume (B, D, F) of the hydrodynamic micelle and cluster average diameters measured at 25, 30 and 37 °C for DHP407 (light blue) and D-DHP407 (dark blue) formulations at 1% w/V polymeric concentration.

3.2. Poly(ether urethane) thermosensitivity evaluation

Due to its amphiphilic nature, Poloxamer® 407 is able to form thermosensitive micellar hydrogels as demonstrated first by Bermudez et al. [43]. Therefore, the presence of P407 as repeating unit in DHP407 backbone ensures the temperature-driven capability of PEU chains to arrange into micelles as assessed in previous works for similar PEUs differing for the chain extender [29,40,44]. In this work, aiming at developing a minimally invasive injectable delivery system suitable for the treatment of hard-to-close skin wounds, PEU thermo-responsiveness was investigated to identify the proper polymer concentration able to give sol-gel systems at approx. physiological temperature. Moreover, we also assessed if the acid treatment performed to expose secondary amines could detrimentally affect this system responsiveness. To this purpose, both DHP407 and D-DHP407 capability to arrange into micelles was first studied at the nano-scale by estimating the temperature-driven variation of micelle hydrodynamic diameter and the Critical Micellar Temperature of PEU-based solutions. Then, system thermo-responsiveness was definitely assessed at the macro-scale through Tube Inverting and Gelation Time tests, allowing the definition of the most promising gelling concentration, which was then rheologically characterized.

3.2.1. Investigation of system thermo-responsiveness at the nano-scale

The temperature-induced micelle arrangement and their changes in the average hydrodynamic diameter upon system heating were first investigated through Dynamic Light Scattering (DLS) measurements performed on both DHP407 and D-DHP407 formulations at different temperatures. Fig. 4 reports the intensity (A, C and E) and the volume (B, D and F) patterns of the polymeric structures contained in PEU formulations at 1% w/V concentration measured at 25, 30 and 37 °C. Considering the patterns by intensity, it was not possible to measure an average hydrodynamic diameter at the lowest tested temperature (i.e., 25 °C, Fig. 4_A), irrespective of the tested polymer. Indeed, the very low stability of the newly formed structures brought to continuous aggregation and disaggregation phenomena, thus suggesting the absence of a clear chain organization [30]. Upon temperature increase up to 30 °C (Fig. 4_C), both DHP407 and D-DHP407 formulations showed two well-defined peaks which can be dimensionally ascribed to micelles and aggregates [27,34]. More in detail, similar average hydrodynamic micelle diameters were registered for DHP407 and D-DHP407 structures (i.e., 34.6 ± 2.6 nm and 39.6 ± 2.4 nm, respectively) meaning that nor the presence of pendant Boc-caging groups neither the acid treatment performed to expose the secondary amines alter the process of temperature-induced micelle formation. Conversely, different average values were measured for micellar clusters, i.e., 211.2 ± 36.2 nm and 310.9 ± 13.5 nm for DHP407 and D-DHP407, respectively. These evidences could be correlated to the superior inclination of amine-exposing micelles to interact with the surrounding medium and aggregate entrapping water molecules, in accordance with data reported on PEU micelles exposing thiol groups [30]. Such bimodal chain organization into micelles and aggregates was further confirmed upon heating up to physiological temperature, with average hydrodynamic diameters measured to be 35.9 ± 1.2 nm - 235.6 ± 19.9 nm and 40.1 ± 5.1 nm - 260.1 ± 20.5 nm for DHP407 and D-DHP407 single micelles and clusters, respectively.

However, considering the volume patterns (Fig. 4_B, D and F) only one peak at about 30 nm was detected, meaning that the amount of aggregates present in the sample was negligible (< 1% for all tested temperatures) compared to that of single micelles.

The temperature-guided chain organization into ordered structures was also assessed by estimating the Critical Micellar Temperature (CMT) upon the addition of a micellization marker (i.e., DPH) to PEU solutions. Specifically, such marker is able to give progressively increasing absorbance values at 356 nm by increasing the amount of micelles entrapping the molecule. The CMT is the temperature at which the measured absorbance firstly increased, meaning that the first micelle appeared. Irrespective of tested polymer, no signals were detected up to 20 °C (data not reported) suggesting the absence of chain organization into core-shell structures, in accordance with previous works [28,34,40]. Further

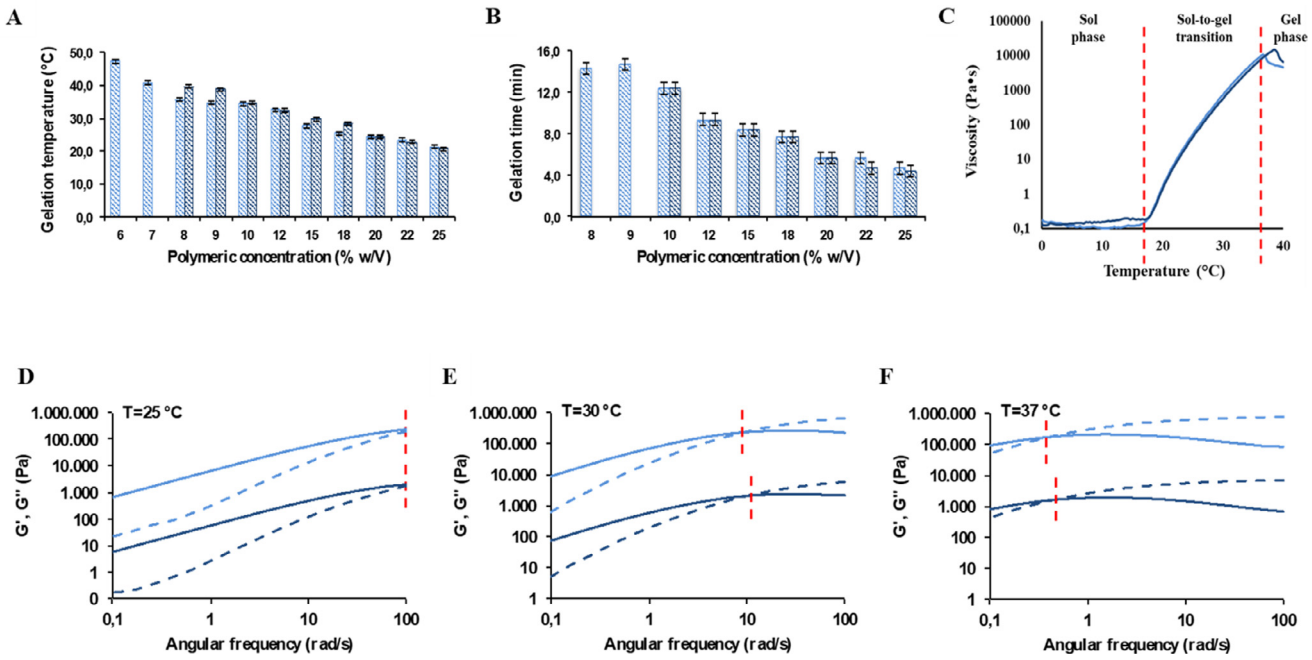

Fig. 5. Tube Inverting Test conducted in temperature ramp (A – range 5–70 °C, 1 °C/step, error ± 0.5 °C) and isothermal (B – 37 °C, 1 min/step, error ± 30 s) conditions by three independent operators on DHP407 (light blue) and D-DHP407 (dark blue) aqueous solutions prepared by dissolving the polymer in physiological saline solution at different concentrations. Viscosity profile *vs.* temperature during the sol-to-gel transition as analyzed through temperature ramp test performed on DHP407 (light blue) and D-DHP407 (dark blue) solutions at 15% w/V concentration (C). Storage (G' – dashed line) and loss (G" – continuous line) moduli registered for DHP407 (light blue) and D-DHP407 (dark blue) formulations at 25 °C (D), 30 °C (E) and 37 °C (F). The red bars identify the crossover frequency between the storage and the loss moduli, i.e., the frequency which marks the beginning of the transition from the sol to the gel state. For clear data interpretation, DHP407 profiles were shifted along the y-axis by multiplying the registered G' and G" values by a factor of 100.

system heating resulted in absorbance intensity increase and thus, in the formation of micelles, in accordance with DLS results. However, although slight differences were registered in the average hydrodynamic diameters of DHP407 and D-DHP407 micelles, no remarkably different CMT values were measured for the analyzed systems (i.e., 22.5 °C and 23.1 °C for DHP407 and D-DHP407, respectively). Hence, such evidences further assessed the retained polymer thermo-responsiveness upon the acid treatment and absence of Boc-dependent effects in the chain organization process.

3.2.1. *Investigation of system thermo-responsiveness at the macro-scale*

The capability of the synthesized PEUs to form hydrogels through a temperature-controlled micelle-driven sol-to-gel transition was first qualitatively studied by means of Tube Inverting tests performed in temperature ramp or isothermal conditions. The former test allowed also the definition of the Critical Gelation Concentration (CGC), i.e., the lowest polymer concentration able to form a solid gel, while the latter gave information about hydrogel gelation time at physiological temperature. According to previous works on similar PEU-based systems [34,35], the gelation temperature of both systems was strictly dependent on the polymeric concentration: upon a decrease in system polymeric content a remarkable increase in the sol-gel transition temperature was observed up to 6% w/V and 8% w/V concentration for DHP407 and D-DHP407 systems, respectively (Fig. 5_A). However, upon further heating up to 70 °C, no other DHP407 and D-DHP407 formulations were able to undergo gelation. Therefore, although the removal of Boc-caging groups did not affect chain capability to arrange into micelles as previously assessed at the nano-scale, it slightly altered the measured CGC of PEU formulations. In addition, this test also revealed that DHP407 and D-DHP407 systems with polymeric concentration lower than 7% w/V and 9% w/V were able to complete the transition from the sol to the gel state at temperatures higher than the physiological value. Hence, these formulations were not considered in the tube inverting test conducted at 37 °C.

Concerning hydrogel gelation kinetics in physiological-like conditions (Fig. 5_B), a decrease in the time required to ensure a complete sol-to-gel transition was observed upon an increase in hydrogel concentration, suggesting that the gelation kinetics was strictly dependent on the polymeric concentration [34,35]. In view of their application as injectable delivery systems for the treatment of chronic skin wounds, the most promising polymer concentration able to undergo gelation at approx. physiological temperature within few minutes turned out to be 15% w/V. Indeed, this formulation showed gelation temperatures of 27.7 ± 0.6 °C and 29.7 ± 0.6 °C for DHP407 and D-DHP407, respectively. On the other hand, no differences were registered in the gelation time, which was measured to be 8.3 ± 0.6 min for both systems.

Therefore, this composition was selected as the optimal condition in terms of thermo-responsiveness and further characterized by rheological tests to definitely assess the temperature-driven hydrogel gelation mechanism at the macro-scale. Hence, temperature ramp within the 0–40 °C range and frequency sweep tests at 25, 30 and 37 °C were conducted on both DHP407 and D-DHP407 sol-gel systems at 15% w/V concentration (Fig. 5_C–F). The temperature ramp profile of thermo-responsive systems characterized by a Lower Critical Gelation Temperature (LCGT) can be subdivided into three main temperature-dependent phases: (i) viscosity decrease, (ii) sharp viscosity increase and (iii) viscosity maintenance (Fig. 5_C). The first phase corresponds to the characteristic behavior of sol systems when subjected to heating, while the second one refers to micelle aggregation and network formation. The temperature and viscosity values that mark the transition from the first to the second phase are characteristic parameters of the gelation process. Indeed, the temperature at the minimum of viscosity (T_{onset}) identifies the temperature at which micelles reach the critical micellar volume required to begin the gelation process [34]. This temperature was measured to be 14.4 °C and 17.0 °C for DHP407 and D-DHP407 systems, respec-

tively. Therefore, the formation of DHP407 micelles and their aggregation into an organized network required lower temperatures to start compared to D-DHP407 ones, according to CMT values measured at the nano-scale. Such different behavior can be probably ascribed to the presence of a pendant hydrophobic moiety along DHP407 chains, which favored their arrangement into micelles, thus reducing the contact with the surrounding water molecules. Beside these initial differences, then the systems behaved similarly during the sol-to-gel transition as the registered profiles were completely overlapped in the second phase. Lastly, the third phase defines the gel state and should be characterized by a temperature-independent viscosity trend. Conversely, both DHP407 and D-DHP407 profiles showed an unexpected viscosity decrease at 36 °C and 38 °C, respectively. However, this behavior was not due to a further transition within the material but rather to network disentanglements resulting from the application of a continuous strain to the samples [35].

In addition, frequency sweep tests performed on both sol-gel systems at different temperatures evidenced similar behaviors in the process of gel formation and development upon heating (Fig. 5_D–F). Hence, such characterization definitely proved that the acid treatment performed to remove Boc-caging groups did not considerably alter D-DHP407 system capability to undergo gelation compared to DHP407 formulations. Based on the conventionally defined relationship occurring between the storage (G') and the loss (G") moduli values [40], the characterized sol-gel systems turned out to be mainly in the sol state at 25 °C, in a biphasic phase at 30 °C and not-completely developed gels at 37 °C. Indeed, the crossover frequencies between G' and G" moduli (i.e., 0.45 rad/s and 0.5 rad/s for DHP407 and D-DHP407, respectively) were registered within the investigated angular frequency range, meaning that a strong relationship between both moduli and the angular frequency still occurs at 37 °C. However, although the gelation process was not completed at physiological temperature, the 15% w/V concentrated formulations were able to give a macroscopically solid gel, in accordance with the qualitative Tube Inverting tests. Such observations were further supported by data obtained from strain sweep tests performed at 37 °C, which provided differences between the storage and loss moduli lower than one order of magnitude (i.e., $\Delta(G'\text{-}G")_{@0.01\%}$= 4.5 kPa and 4.1 kPa for DHP407 and D-DHP407 gels, respectively) (Fig. S7). However, although both systems showed a similar degree of network development, remarkably different critical deformations (i.e., the strain values at the end of the linear viscoelastic region) were measured at physiological temperature, i.e., 11.6% and 18.6% for DHP407 and D-DHP407, respectively. This different capability to withstand applied deformation can be attributed to a different network organization in the presence of exposed secondary amino groups. Specifically, the presence of these hydrophilic functional groups enhances the formation of H-bonds between micelles and stronger interactions between them and the surrounding water molecules. Hence, such additional "bridges" finally led to the achievement of a more resistant hydrogel network compared to that of DHP407 formulation, in accordance with previous results on hydrogels exposing carboxylic groups along PEU chains [35].

3.3. *In vitro assessment of hydrogel releasing capability and biological performances*

The suitability of the engineered hydrogels as multifunctional formulations for the treatment of infected chronic wounds was *in vitro* investigated in accordance with the 3R (refinement, reduction, replacement) principles. Specifically, system releasing capability was tested by studying the release profile of a model protein; then, their injectability and shape maintenance were assessed in simulated physiological conditions and lastly, system biological performances in their perspective application as wound treatments were proved by means of antimicrobial/antibacterial tests and compatibility tests performed in accordance with the ISO 10993-5 regulation.

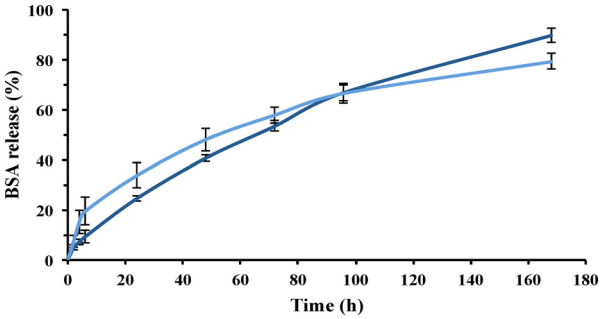

Fig. 6. *In vitro* Bovine Serum Albumin release profiles obtained by incubating DHP407 (light blue) and D-DHP407 (dark blue) hydrogels (15% w/V polymeric concentration) with Phosphate Buffered Saline solution (pH 7.4) at 37 °C for different time points up to 7 days.

3.3.1. *In vitro Bovine Serum Albumin release study*

In view of hydrogel application in the management of hard-to-close skin wounds for the *in situ* release of drugs/biomolecules, Bovine Serum Albumin (BSA) was selected as model protein. Indeed, the main objective was to evaluate the feasibility to potentially deliver hydrophilic molecules characterized by different molecular weights, such as low molecular weight agents (e.g., Adenosine [45]), growth factors (e.g., Vascular Endothelial Growth Factor [46]) and high molecular weight Platelet-Reach Plasma (PRP) [47–49]. To this purpose BSA was loaded at 1 mg/mL concentration in DHP407 and D-DHP407 hydrogels and its release profile was evaluated up to 7 days in physiological-mimicking conditions (Fig. 6). Both systems were able to avoid burst release phenomena and successfully deliver their payload over time, in agreement with previous results obtained on similar PEU-based hydrogels releasing anti-inflammatory drugs [35,50]. In detail, after 24 h of incubation, the released BSA was measured to be 33.7 ± 5.0% and 24.6 ± 1.2% of the total loaded amount for DHP407 and D-DHP407 systems, respectively. However, slight differences were observed in drug release kinetics, probably ascribed to the differences in gel network organization and strength (according to the previously reported rheological considerations) and BSA electrostatic interaction with hydrogel material. More in detail, the formation of a stronger D-DHP407 gel network and the enhanced –NH-mediated BSA/polymer interactions could initially slightly hinder payload release, in accordance with findings on PEU hydrogels encapsulating Ibuprofen Sodium Salt [27]. However, after 4 days of incubation, an inversion in BSA release trend was recorded with released amounts from D-DHP407 hydrogels becoming significantly higher than those from DHP407 systems. Such observation can be explained considering the overall higher hydrophilicity of D-DHP407 formulations, causing higher absorption of watery medium (as reported in a previous work on similar formulations [29]) and consequently, the release of higher amounts of payload compared to DHP407 hydrogels. More in detail, within the first time points of incubation, the stronger D-DHP407 gel network decreased its swelling capability; however, when the medium began to considerably infiltrate the network, progressive dissolution phenomena prevailed over the system stability, resulting in released BSA amounts significantly higher compared to DHP407 systems (i.e., 79.2 ± 3.1 and 89.7 ± 2.7% for DHP407 and D-DHP407, respectively, after 7 d of incubation). As the polymeric concentration was the same, such differences in release kinetics were attributed to the presence of exposed hydrophilic secondary amino groups and superior hydrophilicity of D-DHP407 than DHP407 hydrogels.

3.3.2. *Evaluation of hydrogel injectability*

Hydrogel injectability was investigated to evaluate system capability to precisely and mini-invasively deliver their therapeutic payload. To this purpose both DHP407 and D-DHP407 formulations were prepared at 15% w/V polymeric concentration and equilibrated at 4, 25 and

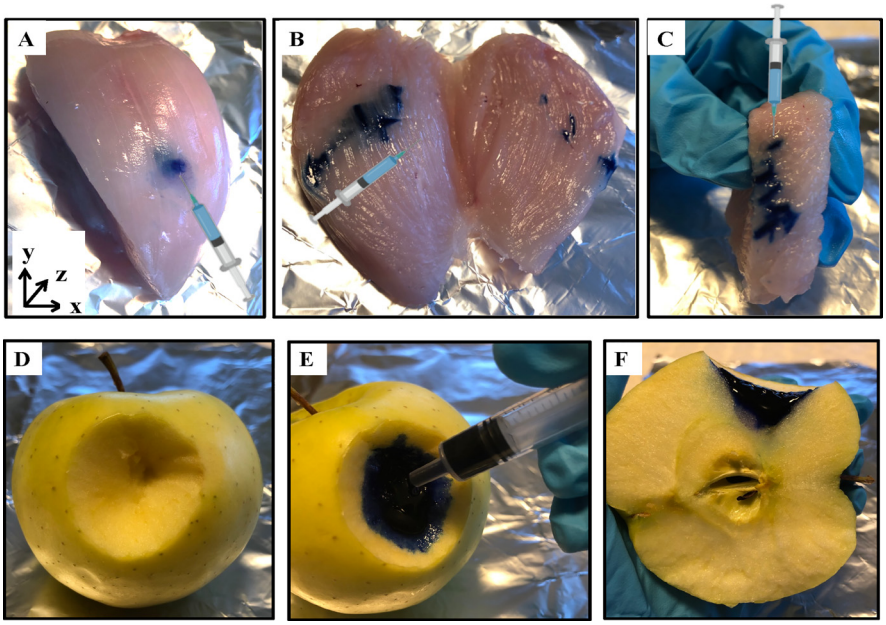

Fig. 7. Qualitative injectability tests performed to evaluate DHP407 and D-DHP407 potentialities as carriers for the mini-invasive or topical administration of drugs/biomolecules in the treatment of hard-to-close skin wounds. Injection of PEU formulations in the sol state through a G21 needle in a piece of chicken meat (A) and cross-sections along y- and z-axes (B and C, respectively) upon incubation for 15 min at 37 °C. Evaluation of hydrogel capability to adapt to the wound morphology (D) upon injection in the sol state (E) and to keep the shape after the sol-to-gel transition (F).

Table 3
Evaluation of DHP407 and D-DHP407 injectability in the sol (4 °C), semi-gel (25 °C) and gel (37 °C) state through needles with different internal diameters.

		Injectability of PEU sol-gel formulations			
		G22	G21	G18	G16
4 °C	DHP407	√	√	√	√
	D-DHP407	√	√	√	√
25 °C	DHP407	√	√	√	√
	D-DHP407	√	√	√	√
37 °C	DHP407	✗	✗	√	√
	D-DHP407	✗	✗	√	√

37 °C to achieve the sol, semi-gel and gel state. Then, at each temperature, injection was performed through needles with different diameters (Table 3).

All tested conditions evidenced an easy injectability of both DHP407 and D-DHP407 formulations. However, too high pressures were required to achieve a continuous flow when injected through G22 and G21 needles at physiological temperature (i.e., in the gel state). Hence, they were considered not injectable in this condition.

Furthermore, to qualitatively evaluate the potential resistance exerted by the tissues during injection, both formulations were also injected in the sol state in a piece of chicken meat (Fig. 7_A) by using a G21 needle. Then, the chicken meat was equilibrated at 37 °C for 15 min and cross sections were performed to assess gelling solution dispersion within the tissues (Fig. 7_B and C). Both systems turned out to be easily injectable in the sol state and able to remain in the injection site upon a quick heating up to physiological temperature as a consequence of their sol-to-gel transition.

Lastly, system potentialities as topical delivery carrier able to exploit temperature changes to adapt to the wound morphology, undergo *in situ* gelling and keep the shape over time were qualitatively assessed (Fig. 7_D). To this purpose, an hole was first made into an apple, then it was filled with the gelling formulation in the sol state and finally, incubated at 37 °C for 15 min (Fig. 7_E). The cross-section performed along the z-axis confirmed the capability of the system to remain in the desired site (Fig. 7_F), thus providing promising results in view of the application such PEU-based systems were designed for.

3.3.3. *In vitro poly(ether urethane) cytocompatibility*

Hydrogel cytocompatibility was assessed according to ISO 10993-5 using NIH-3T3 murine fibroblasts and a multiplex assay to simultaneously evaluate cell cytotoxicity and cell viability (Fig. 8_A and B). To this purpose, cells were cultured for 24 h in the presence of hydrogel extracts and in complete medium as control condition. Results showed no cytotoxicity (Fig. 8_A). On the other hand, the metabolic activity of cells cultured for 24 h in the presence of D-DHP407 extracts was similar to the control (i.e., 92.8% ± 4.2%), while that of cells in contact with DHP407 extracts was significantly lower evidencing non-cytocompatibility of DHP407 hydrogel (Fig. 8_B). Indeed, although DHP407 extracts did not directly provoke cell membrane disruption, they progressively induced cells to achieve a quiescent condition. The different behavior of the extracts was attributed to changes in PEU hydrophobic/hydrophilic balance after deprotection. The removal of the hydrophobic Boc-protecting group caused the exposure of hydrophilic –NH functionalities, increasing overall PEU hydrophilicity. Thus, after deprotection, any PEU chains dissolved in the extracts showed reduced capability to interfere with cell membranes.

Furthermore, to evaluate whether gel extracts could potentially affect cell proliferation, cells were cultured in extract-enriched media or complete medium (as control condition) for different time points up to 72 h. At each time interval, cells were lysed and the concentration of released lactate dehydrogenase (LDH) was quantified through the CytoTox-ONE™ assay. Cell proliferation was reported by referring the amount of released LDH at each time point to the initial time, i.e., 24 h after seeding and before the addition of hydrogel extracts (Fig. 8_C and D). Cells treated with DHP407 extracts showed no proliferation capability and poor metabolic activity from 24 to 72 h culture time. Furthermore, cells appeared round-shaped as an evidence of a non-viable status (Fig. 8_C and D). On the contrary, cells treated with D-DHP407-enriched medium showed an increasing proliferation rate up to 48 h that was measured not to be statistically different compared to the control, as further supported by bright-field images of cell morphology (Fig. 8_C and D). Therefore, although a slight reduction in the proliferation trend was observed after 3 days, D-DHP407 extracts did not affect NIH-3T3 proliferation capability, thus providing promising preliminary results in view of future hydrogel use in wound healing applications.

3.3.4. *In vitro poly(ether urethane) antimicrobial activity*

Based on the literature, to exert a remarkable antimicrobial activity, engineered antimicrobial polymers should show specific features, such as amphiphilicity, high molecular weight and exposure of positively charged functional groups to improve polymer interaction with

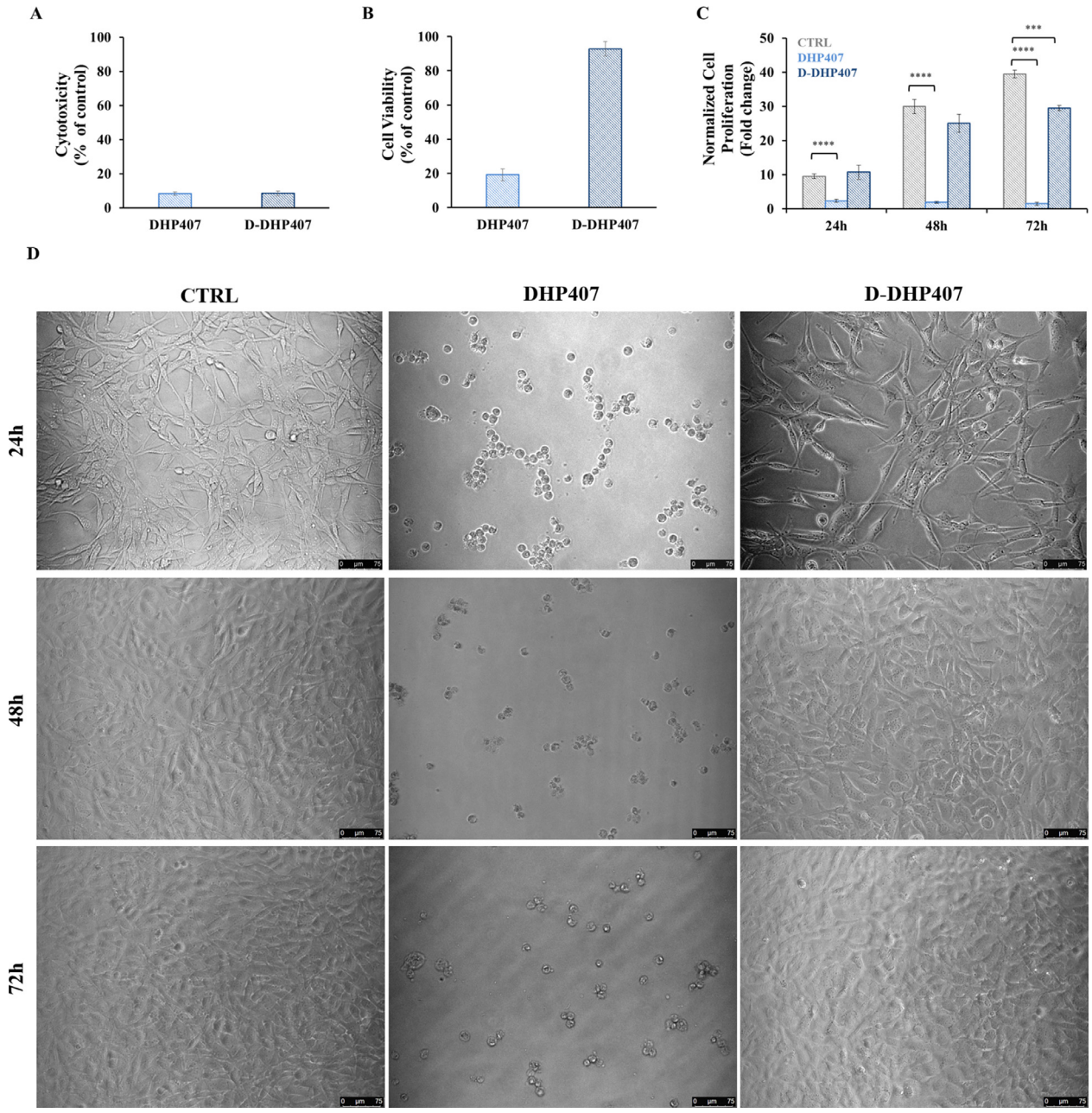

Fig. 8. Biocompatibility evaluation of hydrogel extracts according to ISO 10993-5. Cytotoxicity of DHP407 (light blue) and D-DHP407 (dark blue) formulations tested through the CytoTox-ONE^{TM} assay and calculated with respect to the positive control (A). Cell viability tested for DHP407 (light blue) and D-DHP407 (dark blue) PEUs through the CellTiter-Blue assay and calculated with respect to cells cultured in normal conditions (B). Proliferation capability of cells treated with complete medium (CTRL, gray) and DHP407 and D-DHP407 extracts (light- and dark-blue, respectively) up to 72 h (C). Cell proliferation was evaluated by referring the concentration of released lactate dehydrogenase at each time point to that of the initial time (i.e., cells cultured for 24 h in normal conditions to allow adherence). Bright-field images of CTRL, DHP407- and D-DHP407-treated cells at 24, 48 and 72 h to visually inspect cell proliferation (D).

the negatively charged bacteria membrane [18–20]. In this work, the antimicrobial activity of the synthesized amphiphilic high molecular weight DHP407 and D-DHP407 PEUs was investigated against standard strains of *S. aureus, P. aeruginosa, E. coli* and *C. albicans,* being the microbial species primarily responsible for infections and biofilm formation in human chronic wounds [1–3]. Specifically, these PEUs differ for the exposure of secondary amino groups along D-DHP407 chains. The same tests were also performed on P407 macrodiol as control condition for polymer amphiphilicity. Fig. 9 shows the optical density of cell suspensions co-incubated for 24 h with different concentrations of the three compounds. The same polymeric formulations were also tested for cytocompatibility to verify that the observed antibacterial activity was ascribed to engineered polymer features rather than to polymer-induced cytotoxic effects (Fig. S8).

In the case of the Gram-positive strain *S. aureus*, P407, DHP407 and D-DHP407 formulations were able to inhibit bacterial growth up to 33%, 78% and 77%, respectively, at 25 mg/mL concentration. DHP407 and D-DHP407 resulted to be more effective compared to P407 ($p < 0.0001$) as a consequence of their higher molecular weight (i.e., $\bar{M}_w$= 33 kDa *vs.* 12 kDa as assessed through SEC analysis). Indeed, as Gram-positive bacteria show a loose cell wall, higher molecular weight polymers are able to more effectively diffuse across and disrupt bacteria membrane compared to lower molecular weight polymers [18,20]. Furthermore, at all tested concentrations, the antimicrobial effect of DHP407 and

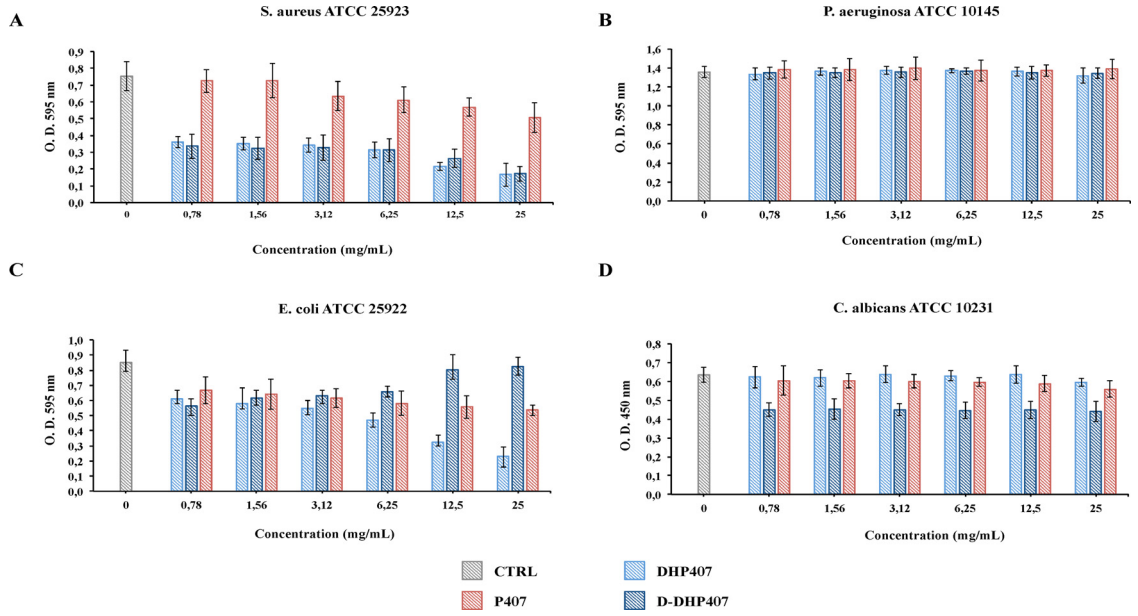

Fig. 9. Antimicrobial activity of the synthesized DHP407 and D-DHP407 poly(ether urethane)s and the amphiphilic P407 macrodiol at 24 h on *S. aureus* (A), *P. aeruginosa* (B), *E. coli* (C) and *C. albicans* (D), measured by optical density.

D-DHP407 was comparable ($p > 0.05$) suggesting that in this case the contribution of exposed secondary amino groups and different hydrophilic/hydrophobic balance on antibacterial activity was negligible.

Differently from Gram-positive bacteria, Gram-negative bacteria are characterized by a double cell membrane, forming an additional barrier against antimicrobial agents/polymers that makes Gram-negative bacteria contamination more difficult to eradicate. Indeed, no antibacterial activity ($p > 0.05$) was detected against the Gram-negative strain *P. aeruginosa*. Conversely, all tested polymers were able to inhibit the growth of the Gram-negative strain *E. coli* in a concentration-dependent manner, with DHP407 formulations being the most effective. Specifically, the highest inhibition was measured at 25 mg/mL concentration for P407 (34%) and DHP407 (75%), and at 0.78 mg/mL concentration for D-DHP407 (32%). Hence, the role exerted by the hydrophobic/hydrophilic balance in DHP407 formulations prevailed over exposure of –NH groups in D-DHP407 ones. Such evidences were further supported by CMC results showing a lower value for DHP407 PEU (i.e., 17.5 μg/mL) compared to P407 and D-DHP407 (i.e., 18.9 μg/mL and 19.7 μg/mL, respectively).

Lastly, concerning *C. albicans,* no antifungal activity was exerted by P407 and DHP407 ($p > 0.05$). Conversely, D-DHP407 was able to counteract fungal growth in a concentration-independent manner with inhibitions in the range of 29–31% ($p < 0.0001$). This result could be attributed to the presence of secondary amino groups in D-DHP407 resulting in some antifungal activity.

4. Conclusion

Antibiotic-free formulations able to tackle infections, avoiding bacteria resistance and promoting tissue regeneration, are highly demanded as systems for the efficient management of chronic skin ulcers. In this research, an injectable thermosensitive drug delivery hydrogel with intrinsic antimicrobial properties was designed for potential application in the mini-invasive treatment of infected hard-to-close wounds. An amphiphilic high molecular weight poly(ether urethane) (PEU) with Boc-protected secondary amino groups was first synthesized from Poloxamer® 407 macrodiol and N-Boc diethanolamine chain extender. Synthesis reaction was optimized with the aim to maximize the chain extension polymerization step. Secondary amino-groups were exposed along PEU chains by acid treatment and the number of –NH groups/chain was quantified ($4.5 \times 10^{20} \pm 1.8 \times 10^{19}$ units/g of polymer). The exposure of –NH groups did not significantly alter thermo-responsiveness, while affected the payload release kinetics and the biological response. In detail, at the nanoscale, the PEU exposing -NH groups formed slightly larger micelles and clusters as a consequence of the repulsion among positively charged amino groups and more favored interactions with surrounding water molecules. However, Critical Micellar Temperature was not affected. The investigation of system thermo-responsiveness at the macro-scale allowed the identification of the most promising hydrogel concentration (i.e., 15% w/V) with sol-gel behavior for application in drug delivery. Although PEU gelling solutions showed similar sol-gel transition kinetics, a slightly stronger gel network was achieved in the presence of –NH groups. Moreover, the different network organization was found to affect the drug release kinetics, suggesting the possibility to exploit this feature as a means to tune drug/biomolecule release.

Concerning the biological response, extracts from Boc-protected PEU hydrogels compromised cell viability and proliferation. However, at lower cytocompatible concentrations, Boc-protected PEU formulations showed a remarkable antimicrobial activity against both Gram-positive (i.e., *S. aureus*) and Gram-negative bacteria (i.e., *E. coli*) as a consequence of their amphiphilic nature and high molecular weight. On the other hand, after deprotection, hydrogels with exposed –NH moieties showed significantly improved biocompatibility (evaluated following ISO 10993-5) and supported fibroblast proliferation similarly to control conditions. Moreover, D-DHP407 formulations showed a strong antimicrobial activity against the Gram-positive *S. aureus*. Furthermore, the presence of –NH, which protonation degree increases with decreasing the pH, improved antifungal activity against *C. albicans*.

Lastly, both PEU formulations were easily injectable through needles of different sizes, and underwent gelling within few minutes in physiological conditions.

Therefore, due to their injectability, intrinsic antifungal ability and antimicrobial properties against Gram-positive bacteria, and ability for gradual and controlled release of their payload, deprotected PEU hydrogels are promising for future exploitation as multi-functional injectable systems for the treatment of hard-to-heal wounds.

Appendix A. Supplementary material

Supplementary figures

Declaration of Competing Interest

The authors declare no competing financial interest.

CRediT authorship contribution statement

Rossella Laurano: Conceptualization, Methodology, Validation, Formal analysis, Investigation, Data curation, Writing – original draft, Visualization. **Valeria Chiono:** Supervision, Writing – review & editing. **Chiara Ceresa:** Investigation, Data curation, Writing – review & editing. **Letizia Fracchia:** Supervision, Writing – review & editing. **Alice Zoso:** Validation, Writing – review & editing. **Gianluca Ciardelli:** Resources, Supervision, Writing – review & editing. **Monica Boffito:** Conceptualization, Methodology, Validation, Investigation, Writing – review & editing, Supervision, Funding acquisition.

Acknowledgments

This research did not receive any specific grant from funding agencies in the public, commercial, or no-for-profit sectors.

Supplementary materials

Supplementary material associated with this article can be found, in the online version, at doi:10.1016/j.engreg.2021.12.001.

References

[1] V.R. Krishnaswamy, D. Mintz, I. Sagi, Matrix metalloproteinases: the sculptors of chronic cutaneous wound, BBA Mol. Cell Res. 1864 (2017) 22020–22227.
[2] S.B. Chaney, K. Ganesh, S. Mathew-Steiner, P. Stromberg, S. Roy, C.K. Sen, D.J. Wozniak, Histopathological comparisons of Staphylococcus aureus and Pseudomonas aeruginosa experimental infected porcine burn wounds, Wound Rep. Regen. 25 (2017) 541–549.
[3] L. Young, Identifying infection in chronic wounds, Wound Pract. Res. 20 (2012) 1–7.
[4] A. Tammelin, C. Lindholm, A. Hambraeus, Chronic ulcers and antibiotic treatment, J. Wound Care 7 (1998) 435–437.
[5] M. Gürgen M, Excess use of antibiotics in patients with non-healing ulcers, EWMA J. 14 (2014) 17–22.
[6] P.G. Bowler, Antibiotic resistance and biofilm tolerance: a combined threat in the treatment of chronic infections, J. Wound Care 27 (2018) 1–5.
[7] J. Wu, Y. Zheng, W. Song, J. Luan, X. Wen, Z. Wu, X. Chen, Q. Wang, S. Guo, *In situ* synthesis of silver-nanoparticles/bacterial cellulose composites for slow-released antimicrobial wound dressing, Carbohydr. Polym. 102 (2014) 762–771.
[8] R. Augustine, N. Kalarikkal, S. Thomas, Electrospun PCL membranes incorporated with biosynthesized silver nanoparticles as antibacterial wound dressings, Appl. Nanosci. 6 (2016) 337–344.
[9] B. Anisha, R. Biswas, K. Chennazhi, R. Jayakumar, Chitosan–hyaluronic acid/nano silver composite sponges for drug resistant bacteria infected diabetic wounds, Int. J. Biol. Macromol. 62 (2013) 310–320.
[10] N. Cai, C. Li, C. Han, X. Luo, L. Shen, Y. Xue, F. Yu, Tailoring mechanical and antibacterial properties of chitosan/gelatin nanofiber membranes with Fe_3O_4 nanoparticles for potential wound dressing application, Appl. Surf. Sci. 369 (2016) 492–500.
[11] M. El-Aassar, N.M. El-Deeb, H.S. Hassan, X. Mo, Electrospun polyvinyl alcohol/pluronic F127 blended nanofibers containing titanium dioxide for antibacterial wound dressing, Appl. Biochem. Biotechnol. 178 (2016) 1488–1502.
[12] R. Raguvaran, B.K. Manuja, M. Chopra, R. Thakur, T. Anand, A. Kalia, A. Manuja, Sodium alginate and gum acacia hydrogels of ZnO nanoparticles show wound healing effect on fibroblast cells, Int. J. Biol. Macromol. 96 (2017) 185–191.
[13] X. Feng, X. Hou, C. Cui, S. Sun, S. Sadik, S. Wu, F. Zhou, Mechanical and antibacterial properties of tannic acid-encapsulated carboxymethyl chitosan/polyvinyl alcohol hydrogels, Eng. Regene. 2 (2021) 57–62.
[14] T. Chalke, K. Sharma, S.K. Nagare, S.S. Jirge, Formulation and evaluation of punica topical gel for its content of gallic acid and anti-microbial study, Int. J. Drug Deliv. Technol. 6 (2016) 75–78.
[15] A. Sadeghianmaryan, Z. Yazdanpanah, Y.A. Soltani, H.A. Sardroud, M.H. Nasirtabrizi, X. Chen, Curcumin-loaded electrospun polycaprolactone/montmorillonite nanocomposite: wound dressing application with anti-bacterial and low cell toxicity properties, J. Biomater. Sci. 31 (2020) 1–9.
[16] A. Pfalzgraff, K. Brandenburg, G. Weindl, Antimicrobial peptides and their therapeutic potential for bacterial skin infections and wounds, Front. Pharmacol. 9 (2018) 1–23.
[17] G.Mc Donnell, A.D. Russell, Antiseptics and disinfectants: activity, action, and resistance, Clin. Microbiol. Rev. 12 (1999) 147–179.
[18] E.R. Kenawy, S.D. Worley, R. Broughton, The chemistry and applications of antimicrobial polymers: a state-of-the-art review, Biomacromolecules 8 (2007) 1359–1384.
[19] A. Arora, A. Mishra, Antibacterial polymers-a mini review, Mater. Today Proc. 5 (2018) 17156–17161.
[20] L. Timofeeva, N. Kleshcheva, Antimicrobial polymers: mechanism of action, factors of activity, and applications, Appl. Microbiol. Biotechnol. 89 (2011) 475–492.
[21] T. Ikeda, S. Tazuke, S. Biocidal polycations, Polym. Prepr. 26 (1985) 226–227.
[22] T. Tashiro, Antibacterial and bacterium adsorbing macromolecules, Macromol. Mater. Eng. 286 (2001) 63–87.
[23] G.J. Gabriel, A. Som, A.E. Madkour, T. Eren, G.N. Tew, Infectious disease: connecting innate immunity to biocidal polymers, Mater. Sci. Eng. R Rep. 57 (2007) 28–64.
[24] A. Silvestri, S. Sartori, M. Boffito, C. Mattu, A.M. Di Rienzo, F. Boccafoschi, G. Ciardelli, Biomimetic myocardial patches fabricated with poly(ε-caprolactone) and polyethylene glycol-based polyurethanes, J. Biomed. Mater. Res. B 102 (2014) 1002–1013.
[25] A.R. Kim, S.L. Lee, S.N. Park, Properties and *in vitro* drug release of pH- and temperature-sensitive double cross-linked interpenetrating polymer network hydrogels based on hyaluronic acid/poly(N-isopropylacrylamide) for transdermal delivery of luteolin, Biol. Macromol. 118 (2019) 731–740.
[26] S.H. Hsiao, S.H. Hsu, Synthesis and characterisation of dual stimuli-sensitive biodegradable polyurethane soft hydrogels for 3D cell-laden bioprinting, ACS Appl. Mater. Interfaces 10 (2018) 29273–29287.
[27] R. Laurano, M. Boffito, Thermosensitive micellar hydrogels as vehicles to deliver drugs with different wettability, Front. Bioeng. Biotechnol. 8 (2020) 1–19.
[28] R. Laurano, M. Boffito, A. Torchio, C. Cassino, V. Chiono, G. Ciardelli, Plasma treatment of polymer powder as an effective tool to functionalize polymers: case study application on an amphiphilic polyurethane, Polymers 11 (2019) 2109–2126 (Basel).
[29] M. Boffito, A. Torchio, C. Tonda-Turo, R. Laurano, M. Gisbert Garzaran, J.C. Berkmann, C. Cassino, M. Manzano, G.N. Duda, M. Vallet Regi, K. Schmidt-Bleek, G. Ciardelli, Hybrid injectable sol-gel systems based on thermo-sensitive polyurethane hydrogels carrying pH-sensitive mesoporous silica nanoparticles for the controlled and triggered release of therapeutic agents, Front. Bioeng. Biotechnol. 8 (2020) 384–408.
[30] R. Laurano, C. Cassino, G. Ciardelli, V. Chiono, M. Boffito, Polyurethane-based thiomers: a new multifunctional copolymer platform for biomedical applications, React. Funct. Polym. 146 (2020) 104413–104422.
[31] C. Ceresa, M. Rinaldi, V. Chiono, I. Carmagnola, G. Allegrone, L. Fracchia, Lipopeptides from *Bacillus subtilis* AC7 inhibit adhesion and biofilm formation of *Candida albicans* on silicone, Antonie Van Leeuwenhoek 109 (2016) 1375–1388.
[32] C. Pradal, K.S. Jack, L. Grøndahl, J.J. Cooper-White, Gelation kinetics and viscoelastic properties of pluronic and α-cyclodextrin-based pseudopolyrotaxane hydrogels, Biomacromolecules 14 (2013) 3780–3792.
[33] P. Alexandridis, J.F. Holzwarth, T.A. Hatton, Micellization of poly(ethylene oxide)-poly(propylene oxide)-poly(ethylene oxide) triblock copolymers in aqous solutions: thermodynamics of copolymer association, Macromolecules 27 (1994) 2414–2425.
[34] M. Boffito, E. Gioffredi, V. Chiono, S. Calzone, E. Ranzato, S. Martinotti, G. Ciardelli, Novel polyurethane-based thermosensitive hydrogels as drug release and tissue engineering platforms: design and *in vitro* characterization, Polym. Int. 65 (2016) 756–769.
[35] R. Laurano, M. Boffito, M. Abrami, M. Grassi, A. Zoso, V. Chiono, G. Ciardelli, Dual stimuli-responsive polyurethane-based hydrogels as smart drug delivery carriers for the advanced treatment of chronic skin wounds, Bioact. Mater. 6 (2021) 3013–3024.
[36] E. Mancuso, C. Tonda-Turo, C. Ceresa, V. Pensabene, S.D. Connell, L. Fracchia, P. Gentile, Potential of manuka honey as a natural polyelectrolyte to develop biomimetic nanostructured meshes with antimicrobial properties, Front. Bioeng. Biotechnol. 7 (2019) 1–13.
[37] C. Ceresa, F. Tessarolo, D. Maniglio, I. Caola, G. Nollo, M. Rinaldi, L. Fracchia, Inhibition of *Candida albicans* biofilm by lipopeptide AC7 coated medical- grade silicone in combination with farnesol, AIMS Bioeng. 5 (2018) 192–208.
[38] M. Boffito, R. Laurano, D. Giasafaki, T. Steriotis, A. Papadopoulos, C. Tonda-Turo, C. Cassino, G. Charalambopoulou, G. Ciardelli, Embedding ordered mesoporous carbons into thermosensitive hydrogels: a cutting-edge strategy to vehiculate a cargo and control its release profile, Nanomaterials 10 (2020) 2165–2189.
[39] E. Yildiz, A. Gungor, H. Yildirim, B.M. Baysal, Synthesis and characterization of UV-curable acrylated urethane prepolymers, Die Angew. Makromol. Chem. 219 (1994) 55–66.
[40] R. Laurano, M. Abrami, M. Grassi, G. Ciardelli, M. Boffito, V. Chiono, Using Poloxamer® 407 as building block of amphiphilic poly(ether urethane)s: effect of its molecular weight distribution on thermo-sensitive hydrogel performances in the perspective of their biomedical application, Front. Mater. 7 (2020) 1–24.
[41] B. Trathnigg, Size-exclusion Chromatography of Polymers, John Wiley Sons Ltd, Chichester, UK, 2000.
[42] P. Lu, S. He, Y. Zhou, Y. Zhang, Adsorption, micellization and antimicrobial activity of formyl-containing cationic surfactant in diluted aqueous solutions, J. Mol. Liq. 325 (2021) 115168–115176.
[43] J.M. Bermudez, R. Grau, Thermosensitive poloxamer-based injectables as controlled drug release platforms for veterinary use: development and *in vitro* evaluation, Int. Res. J. Pharm. Pharmacol. 1 (2011) 109–118.
[44] M. Boffito, A. Grivet Brancot, O. Lima, S. Bronco, S. Sartori, G. Ciardelli, Injectable thermosensitive gels for the localized and controlled delivery of biomolecules in tissue engineering/regenerative medicine, Biomed. Sci. Eng. 3 (2019) 9–19.
[45] L. Sun, L. Fan, F. Bian, G. Chen, Y. Wang, Y. Zhao, Mxene-integrated microneedle patches with innate molecule encapsulation for wound healing, Research 2021 (2021) 1–9.
[46] P. Losi, E. Briganti, C. Errico, A. Lisella, E. Sanguinetti, F. Chiellini, G. Soldani, Fibrin-based scaffold incorporating VEGF- and bFGF-loaded nanoparticles stimulates wound healing in diabetic, Acta Biomater. 9 (2013) 7814–7821.
[47] H.S. Yang, J. Shin, S.H. Bhang, J.Y. Shin, J. Park, G.I. Im, C.S. Kim, B.S. Kim, Enhanced skin wound healing by a sustained release of growth factors contained in platelet-rich plasma, Exp. Mol. Med. 43 (2011) 622–629.

[48] D.W. Long, N.R. Johnson, E.M. Jeffries, H. Hara, Y. Wang, Controlled delivery of platelet-derived proteins enhances porcine wound healing, J. Control. Release 253 (2017) 73–81.
[49] R. Spanò, A. Muraglia, M.R. Todeschi, M. Nardini, P. Strada, R. Cancedda, M. Mastrogiacomo, Platelet-rich plasma-based bioactive membrane as a new advanced wound care tool, J. Tissue Eng. Regerative Med. 12 (2018) e82–e96.
[50] M. Boffito, C. Pontremoli, S. Fiorilli, R. Laurano, G. Ciardelli, C. Vitale-Brovarone, Injectable thermosensitive formulation based on polyurethane hydrogel/mesoporous glasses for sustained co-delivery of functional ions and drugs, Pharmaceutics 11 (2019) 501–521.